Density Modulated Semi-Packed Micro Gas Chromatography Columns

Ryan Chan

Thesis submitted to the faculty of the Virginia Polytechnic Institute and State University in partial fulfillment of the requirements for the degree of

Master of Science

In

Electrical Engineering

Masoud Agah, Co-chair

Mantu K. Hudait, Co-chair

Xiaoting Jia

May 3rd, 2018

Blacksburg, VA

Keywords: micro gas chromatography, semi-packed, density modulated

Density Modulated Semi-Packed Micro Gas Chromatography Columns

Ryan Chan

ABSTRACT

With the continued evolution of MEMS-based gas chromatography, the drive to develop new standalone systems with lower power consumptions and higher portability has increased. However, with improvements come tradeoffs, and trying to reduce the pressure drop requirements of previously reported semi-packed columns causes a significant sacrifice in separation efficiency. This thesis covers the techniques for evaluating the separation column in a gas chromatography system as well as the important parameters that have the most effect on a column's efficiency. Ionic liquids are introduced as a stable and versatile stationary phase for micro separation columns. It then describes a MEMS-based separation column design utilizing density modulation of embedded micro-pillars which attempts to optimize the balance between separation efficiency and pressure drop.

Density Modulated Semi-Packed Micro Gas Chromatography Columns

Ryan Chan

GENERAL ABSTRACT

Gas chromatography is a technique used by scientists to separate and identify chemical compounds present in a given test mixture. It is a versatile technique that can be used for qualitative and quantitative analysis of complex mixtures in a variety of applications. However, typical gas chromatography systems are confined to a lab because they are large and consume a lot of power. In order to overcome these problems, different research groups have focused their attention towards the development of portable MEMS-based gas chromatography systems. By miniaturizing the various components of a gas chromatography system, these two main issues can be alleviated. This thesis covers the strategies used to develop and evaluate the separation column of a gas chromatography system and introduce a new MEMS-based column design that will further reduce the power consumption.

Acknowledgements

I would like to use this space to direct my thanks to the people that have helped me get to this point.

To Dr. Masoud Agah, I would not be at Virginia Tech if not for an email that I received from him extending an offer to work in the VT MEMS Lab. If not for him earnestly pushing me along the way, I would not have been able to cope with the work and transition to the graduate student lifestyle. He has provided me guidance for when I needed it and I cannot express how helpful he has been as an advisor.

To the staff working in Whittemore Hall, I have always been appreciative of their help and words of encouragement. Mr. Donald Leber has always been someone that I could ask advice of when something arose during fabrication and Mr. Rick Johnston has provided insight on how I should live my life and apply it to its fullest.

To my friends and lab mates, past and present, for always creating a fun work environment. We became a family whether we wanted to or not. Shout outs to Ben Conlon for being the first friend I made after moving from New York and Daniel Herrera for showing me that there are others out there that share my stupid hobbies. Being able to talk about things other than research really allowed me to decompress when things seemed too stressful.

And lastly, to my family for exposing me to engineering as a child and always believing in me and my ability. I wouldn't be here if it weren't for them.

Table of Contents

List of Figures

List of Tables

1. Introduction

In the field of analytical chemistry, gas chromatography (GC) is regarded as the most widely used analytical technique that scientists use to detect and measure volatile organic compounds (VOCs) and semi-volatile organic compounds in an environment [1,2]. These VOCs are generally toxic and can be found in any number of standard day to day products [3]. These include styrene which can be present in polystyrene containers or cigarettes, and benzene which can be found in gasoline or car exhaust. Exposure to low levels of VOCs may not show immediate effects, but repeated exposure, even at low concentration levels, may cause unwanted side effects. Unfortunately, those most at risk to these VOCs generally come in contact with them due to their work environment. In order to protect these people who have the highest exposure, federal laws have been placed to regulate the concentration of these VOCs in an environment. In addition to these toxic compounds, GC is also used to detect non-toxic compounds such as foods, pharmaceuticals, breath biomarkers, plant emissions, and so on [4–6]. These are also applications in which GC can be used to allow for regulating and limiting VOC exposures.

Chromatography, as a technique, was developed in the early 1900's separately by Ramsey and Michael Tswett [7,8]. At its core, chromatography is simply the separation of a sample's internal components through the use of two phases: the first being the mobile phase which carries the sample and the second is the stationary phase in which the separation occurs. Tswett first showed this phenomenon by separating plant pigments using liquid chromatography (LC), and the working principle of GC is similar to LC. In the case of GC, the gas sample to be separated is vaporized and injected into a carrier gas which acts as the mobile phase. This mixture is then passed through a separation column (SC) which has a coating that promotes adsorption (or absorption) and desorption between the injected sample and the column. This coating is also known as the stationary phase. As the sample travels along the SC, the individual compounds partition between the mobile and stationary phases. Depending on the amount of interaction that a compound has with the stationary phase, it may move faster or slower than the other compounds making up the sample which results in separation being achieved.

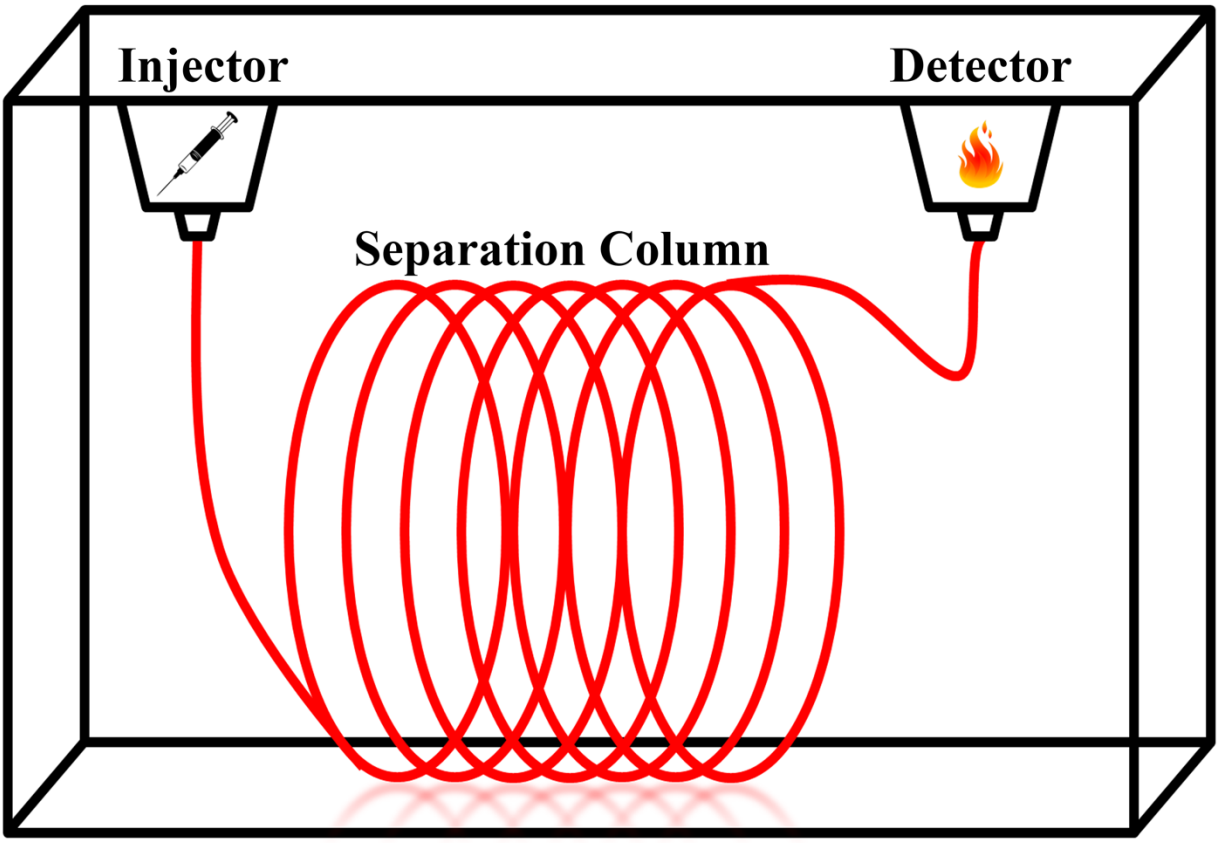

Figure 1.1: Representation of a gas chromatographic system.

A traditional GC tool consists of three major components shown in Figure 1.1. The first that is required is the injector and inlet which handle vaporizing a sample and injecting it into the carrier gas. The inlet controls the temperature that the sample is vaporized at and the pressure that is applied to the inlet of the column while the injector determines whether a sample uses a split or split-less injection. After injection, the sample passes through the separation column which can be considered the most important component of a GC tool. In traditional GC, there are two major variations of separation columns that are used. They are the open tubular column and the packed column. Specifically, the wall coated open tubular column (WCOT) is essentially just a capillary, the walls of which have been coated with a stationary phase. These separation columns range in

length varying anywhere from 10m to up to 200m depending on the application [6,9,10]. The other type of column used in traditional GC is the packed column. Unlike their open tubular counterpart, these columns are generally much shorter with larger inner diameters. Most importantly, they have packing inside which may or may not be coated themselves with a stationary phase. Each of these types of columns provide different advantages over the other with a final decision usually being left up to the application and type of separation that is required. The third and final component that is required is the detector. This part is what generates the chromatogram for data analysis. When it comes to GC detectors, there are certainly a variety to choose from including the flame ionization detector, the thermal conductivity detector, the photoionization detector, as well as some more unconventional including the bubble detector [11].

As technology has matured, the desire to miniaturize platforms has been exhibited all across the board. Some notable examples include the personal computer as well as the telephone. It has also affected GC and as a result, micro gas chromatography (uGC) was developed. These new systems required far less power to operate as well as reduced the amount of time required to run an analysis [12]. They were also much more portable than a traditional tabletop lab tool as some only took up the amount of space a shoebox would [12,13]. This allows for systems to be utilized in the field for real-time analysis or point-of-care use without having to bring samples back to a lab. However, work is constantly being done in an effort to reduce the power consumption for these systems and time required for analysis in an attempt to continue miniaturization and portability.

This work provides a new take on the MEMS-based separation columns that have been previously reported in order to further reduce the power requirements for any GC system. This

includes changes to the topography of the MEMS column as well as the stationary phase used to coat it. These new advances will show the decrease in pressure drop required by the separation column as well as the increased overall flow resulting in faster separations.

1.1. References

[1] H. M. McNair and E. J. Bonelli, "Basic gas chromatography," 1969.

[2] R. L. Grob and E. F. Barry, *Modern practice of gas chromatography*. John Wiley & Sons, 2004.

[3] J. Kesselmeier and M. Staudt, "Biogenic Volatile Organic Compounds (VOC): An Overview on Emission, Physiology and Ecology," *J. Atmospheric Chem.*, vol. 33, no. 1, pp. 23–88, May 1999.

[4] M. Phillips *et al.*, "Volatile organic compounds in breath as markers of lung cancer: a cross-sectional study," *The Lancet*, vol. 353, no. 9168, pp. 1930–1933, Jun. 1999.

[5] L. A. Wallace *et al.*, "Personal exposure to volatile organic compounds: I. Direct measurements in breathing-zone air, drinking water, food, and exhaled breath," *Environ. Res.*, vol. 35, no. 1, pp. 293–319, Oct. 1984.

[6] C. Deng, J. Zhang, X. Yu, W. Zhang, and X. Zhang, "Determination of acetone in human breath by gas chromatography–mass spectrometry and solid-phase microextraction with on-fiber derivatization," *J. Chromatogr. B*, vol. 810, no. 2, pp. 269–275, Oct. 2004.

[7] M. Tswett, "Adsorption analysis and chromatographic method. Application to the chemistry of chlorophyll," *Ber Deut Bot. Ges*, vol. 24, pp. 385–393, 1906.

[8] H. H. Strain and J. Sherma, "M. Tswett: 'Adsorption analysis and chromatographic methods: Application to the chemistry of chlorophylls,'" *J. Chem. Educ.*, vol. 44, no. 4, p. 238, Apr. 1967.

[9] P. Delmonte, A. R. Fardin-Kia, and J. I. Rader, "Separation of Fatty Acid Methyl Esters by GC-Online Hydrogenation × GC," *Anal. Chem.*, vol. 85, no. 3, pp. 1517–1524, Feb. 2013.

[10] "GC Analysis of a 38-Component FAME Mix on SP™-2560, 200 m Column," *Sigma-Aldrich*. [Online]. Available: https://www.sigmaaldrich.com/technical-documents/articles/analytical-applications/gc/gc-analysis-of-a-38-component-fame-mix-g1006572.html. [Accessed: 17-Apr-2018].

[11] A. Bulbul and H. Kim, "A bubble-based microfluidic gas sensor for gas chromatographs," *Lab. Chip*, vol. 15, no. 1, pp. 94–104, 2015.

[12] A. Garg *et al.*, "Zebra GC: A mini gas chromatography system for trace-level determination of hazardous air pollutants," *Sens. Actuators B Chem.*, vol. 212, pp. 145–154, Jun. 2015.

[13] S. Zampolli *et al.*, "Real-time monitoring of sub-ppb concentrations of aromatic volatiles with a MEMS-enabled miniaturized gas-chromatograph," *Sens. Actuators B Chem.*, vol. 141, no. 1, pp. 322–328, Aug. 2009.

2. Background Information

2.1. Separation Column

When it comes to GC tools, the most important part is the separation column. The combination of stationary phase, stationary phase thickness, length of the column, and inner diameter of the column are what determine a separation's efficiency [1,2]. The other defining feature is the type of column that is being used. The two variations include open tubular, which as it implies is a capillary with a circular inner diameter, and packed columns which have a larger inner diameter to accommodate packing beads. The cross-sectional views of these two columns are shown in Figure 2.1. The first columns developed were the packed columns [3]. These columns were typically made of stainless steel and were anywhere from two to ten feet long with an inner diameter of 0.125 to 0.25 inch. They were then filled with what is called a solid support. These solid supports were usually chosen because of their high surface area and inertness and were then coated with a liquid stationary phase. Open tubular columns were not widely used until 1980. Unlike the packed columns, these open tubular columns were much smaller in diameter and did not have any packing inside. This required the stationary phase to be coated on the inside wall of the capillary, and combined with the fact that they were open, allowed for much longer columns due to the lower flow resistance. The advantage that this provided was that these columns were able to completely separate much more complex mixtures than their packed column predecessors

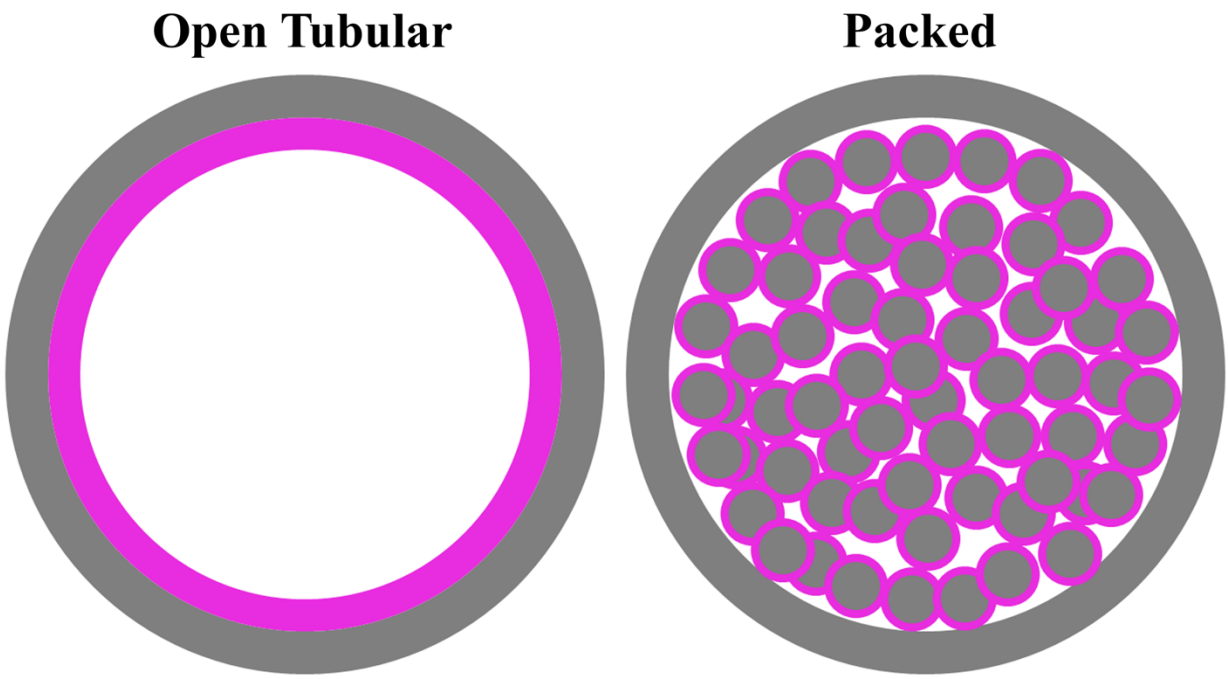

Figure 2.1: Cross-sectional view for open-tubular and packed columns.

[3]. As GC continues to be a very important tool for analytical chemists, countless breakthroughs have been made regarding the columns that are used. These range from characterizing stationary phase for specific applications, as well as inner diameter of the capillary for open tubular columns, and the solid supports that are used in packed columns.

2.2. Stationary Phase

In traditional GC, separation columns are generally identified and categorized based on their stationary phases. This is because, typically, the choice of stationary phase is what determines the efficiency of the separation column. As the test sample traverses the separation column, it comes in contact with the stationary phase that is within. Depending on the amount of interaction that occurs, the individual compounds will start to adsorb and desorb at different rates than the others.

Compounds that spend more time in the mobile phase will pass through the column at a faster rate than one that spends more time in the stationary phase. This leads the compounds to dissociate and elute at different times. Figure 2.2 shows an example of this process through different snapshots in time. As such, the type of column used does not matter if the stationary phase used does not

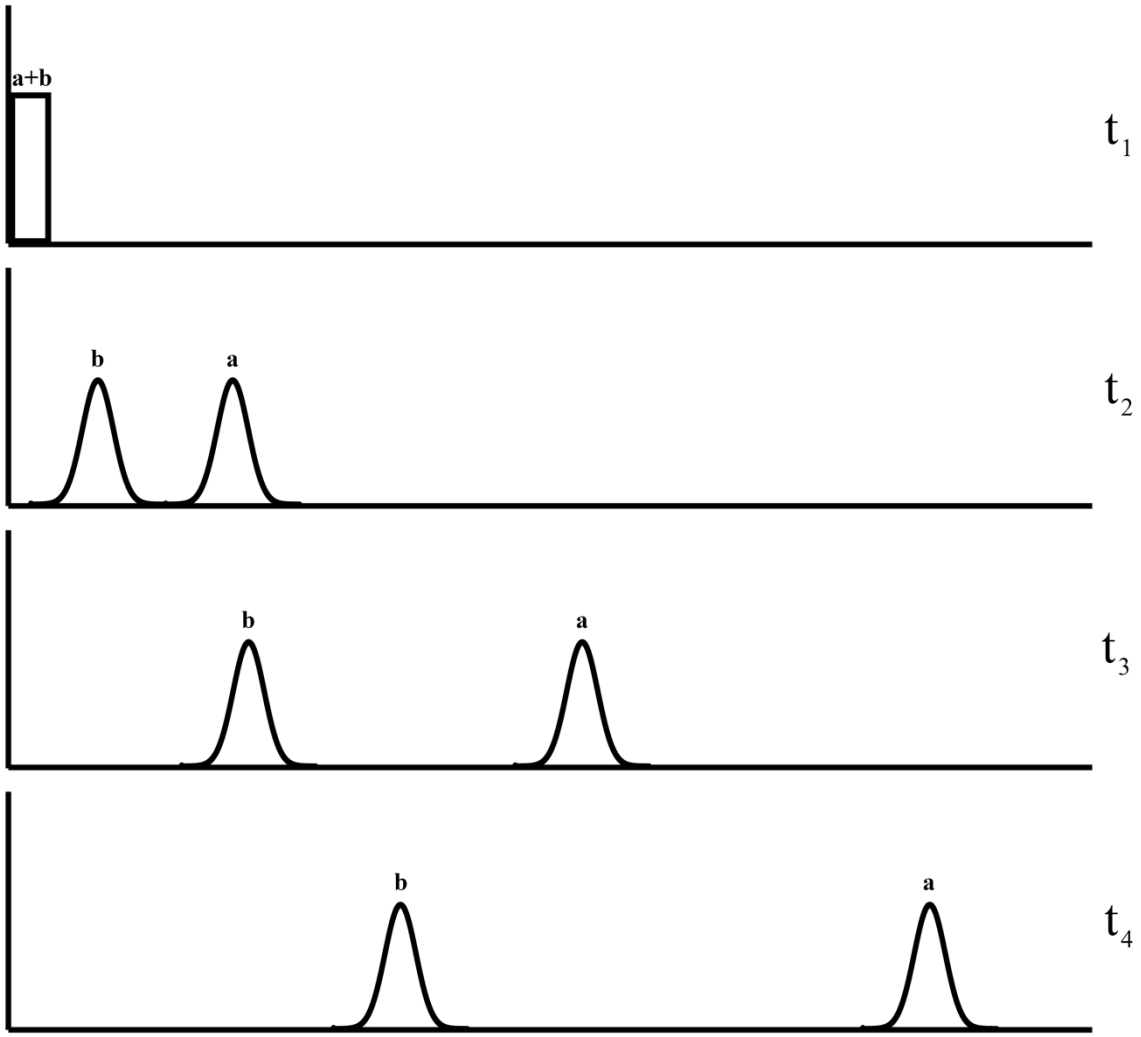

Figure 2.2: Graphical representation of two peaks dissociating during a typical separation. Peak (a) has less interaction with the separation column and therefore travels faster through the column than peak (b).

interact well with the samples that are trying to be separated. For example, a nonpolar stationary phase may not work at all in separating a polar test sample whereas the same sample might completely separate in a polar stationary phase. The stationary phase is also responsible for the elution order of the separated compounds [4]. Commonly used stationary phases include the non-polar OV-1, also known as polydimethyl siloxane (PDMS), and polar Carbowax 20M, also known as polyethylene glycol (PEG). Within these two groups there are also variations that have been developed to better separate compounds for specific applications. However, these traditional materials that are used have drawbacks that include those previously mentioned. One solution to this problem is through the use of room temperature ionic liquids (RTILs). Ionic liquids have been shown to be capable stationary phase coatings for separation columns [5]. Unlike traditional phases such as OV-1, some ionic liquids have the ability to separate both polar and nonpolar compounds [6,7]. This is due to an increased number of solute-solvent interactions versus a traditional phase [8]. Within the category of ionic liquids, it is estimated that there are around a million pure ionic liquids with 10^{18} ternary mixtures possible [9]. This, coupled with the fact that ionic liquids have more ways of interacting with a test sample, leaves a lot of possibility with regards to tuning for specific applications.

2.3. Evaluation of Separation Columns

Before any physical designs are discussed, however, the method of which these columns are evaluated must be discussed. When a separation occurs and a chromatogram is generated, there are a number of factors that must be taken into consideration in order to ascertain the performance of the separation column. At a high level, they are the resolution of the peaks, the symmetry of the

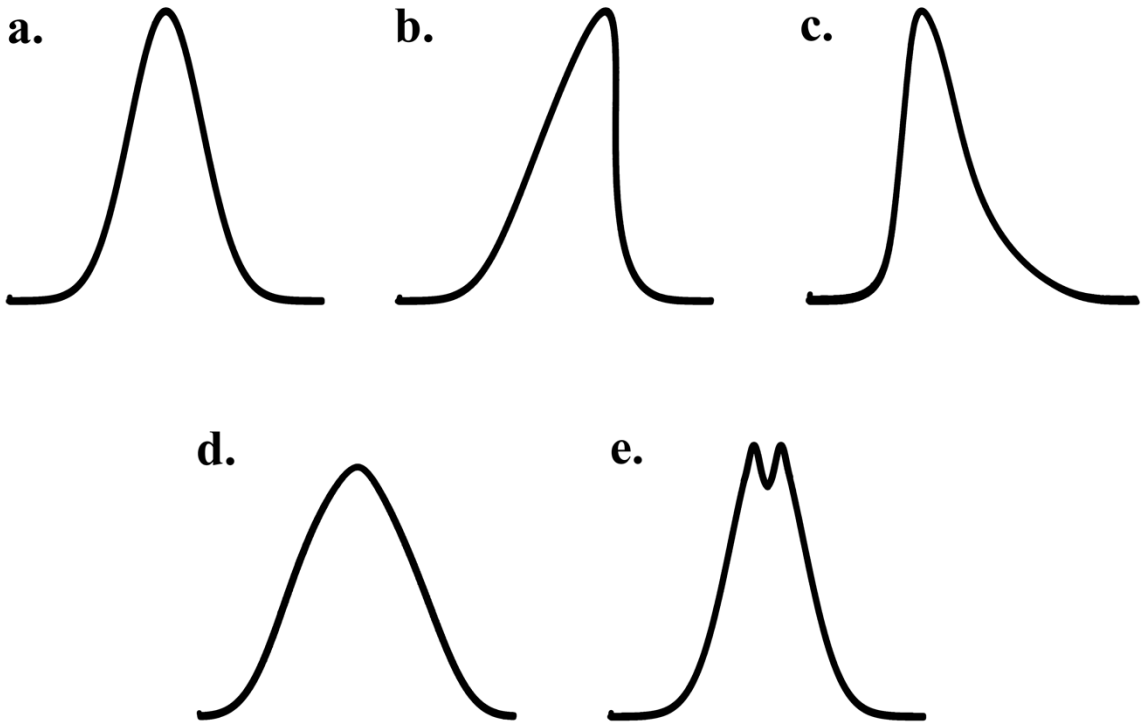

Figure 2.3: Different peak shapes. (a) ideal peak, (b) fronting, (c) tailing, (d) peak broadening, (e) double peak. Peaks (b) through (e) are all undesirable and can be due to a number of reasons, including but not limited to: poor column/stationary phase selection, sample injection volume, or average carrier gas velocity.

peaks, and the sharpness of the peaks. Ideally, the peak should have a Gaussian shape. Examples of peak shapes are shown in Figure 2.3. There are several factors that can contribute to the shape of the peaks straying from the ideal, but are generally due to the interaction between the analyte and the separation column. However, it is not enough to simply look at a chromatogram to evaluate its performance as that is not quantitative. In order to do so, the plate number is used calculate a numerical efficiency value for a separation column:

$$N = 5.54 \left(\frac{t_r}{w_h}\right)^2$$

where N is the plate number, t_r is the retention time of the peak, and w_h is the width of the peak at the half-height. As plate number can change based on the retention time, it is usually

calculated using a single compound under isothermal conditions. Standard practice is to use a compound with a capacity factor greater than five. Capacity factor is described as:

$$k = \frac{t_r - t_m}{t_m}$$

where k is capacity factor and t_m is the retention time of methane. Methane is chosen because it is unretained as a compound by the separation column. As k increases in value, it indicates that the compound that is being used has a greater interaction with the separation column resulting in a more meaningful plate number calculation. After the plate number is calculated there is a normalization that occurs which is known as the plate height:

$$H = \frac{L}{N}$$

where H is the plate height and L is the length of the column. This is the value that most evaluators will look at in order to determine the performance of a separation column. A more efficient column will have a large value for N and a small value for H. This plate height number can then be used to characterize a separation column with what is called a Van Deemter Plot. It is built by plotting the plate height number as a function of velocity and can be seen in Figure 2.4. This graph allows a user to identify the optimal mobile phase velocity for a given separation column as the lowest point on the curve indicates where the column operates at its most efficient. This graph is a great way to compare columns against one another.

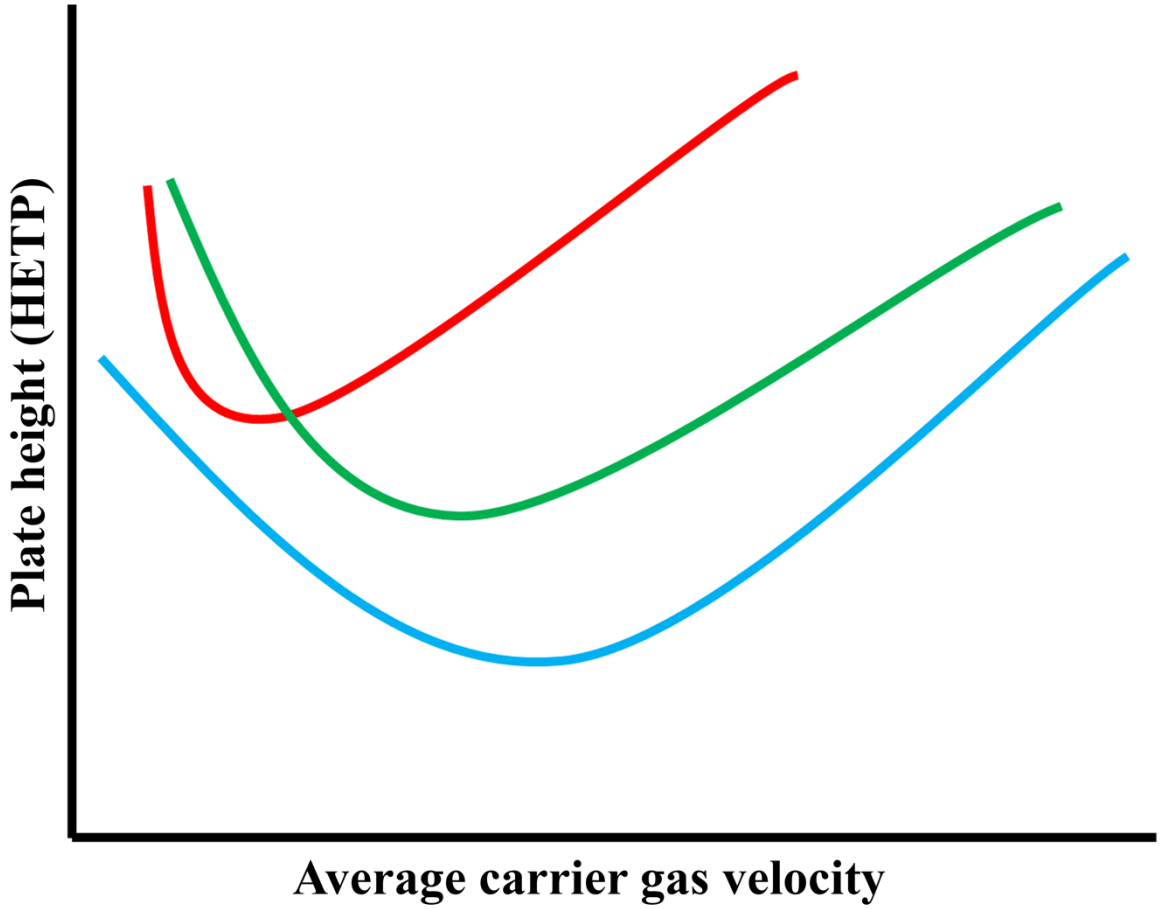

Figure 2.4: Van Deemter Plot showing different column plate heights based on average carrier gas velocity. The lowest point on each curve corresponds to the ideal average carrier gas velocity to achieve maximum separation efficiency. This allows for easy comparisons between different columns.

2.4. MEMS-based GC

As GC technology has matured, so too has other fields. Technology is becoming ever more miniaturized in order to be less intrusive and more portable for everyday use. While transistors are constantly getting smaller leading to more compact electronics, there are mechanical systems that are following suit. This has led to the introduction of micro-electrical mechanical systems (MEMS) as a means to fabricate accompanying systems on a micro-scale. The first published works

concerning MEMS-based GC were back in the 1970's by a group out of Stanford University [10]. It detailed an instrument based on silicon as a substrate with an etched sample loop, separation column, and thermal conductivity detector. This first system performed poorly, however, with the column portion eventually being removed in favor of a traditional wall coated open tubular column to continue their analysis. Since then, there have been a number of advancements made in the development of MEMS-based GC systems both in the form of miniaturizing the entire GC system for portability and power reduction [11,12] and each specific component, be it the pre-concentrator, separation column, or detector [13–17]. As this work pertains to the separation column specifically, they will be explained in more detail.

MEMS-based separation columns for GC, or micro-separation columns (uSC), have been evolving ever since they were introduced. Similar to traditional GC, there are now a variety of different uSCs configurations that have been developed by companies and university research groups. The most common substrate to fabricate these columns on is silicon because of its universal understanding from a cleanroom perspective. Standard photolithography steps are followed, including spinning photoresist and exposing using a mask to create the patterns for the separation column. At this point, the silicon is ready to be etched in order to create the microfluidic channels. Both wet and dry etching have been used to create uSC, with each technique creating unique cross sections depending on the etch parameters. Examples of these can be seen in Figure 2.5. After etching the channels, they need to become airtight. This can be achieved through a few different ways. The first is to deposit a material that closes up the top of the channels created through etching. This is most commonly seen in channels that have been created using an isotropic etch and is also known as buried channel technology [18] which can be seen in Figure 2.6a. The other type of channel is generated by using an anisotropic etch, generally through the use of deep reactive

ion etching. As opposed to channels created using an isotropic etch, anisotropic etches create very vertical sidewalls resulting in channels with a rectangular cross section, as seen in Figure 2.6b. The process to create these types of channels is similar to the previous style in that photoresist is first spun and standard photolithography steps take place. However, once the etching is complete, a second substrate is bonded to the face of the processed silicon wafer to create the airtight seal as the technique used in anisotropic etching will not work. This is generally done by bonding a Pyrex wafer to the silicon through a technique known as anodic bonding. By applying heat, pressure, and

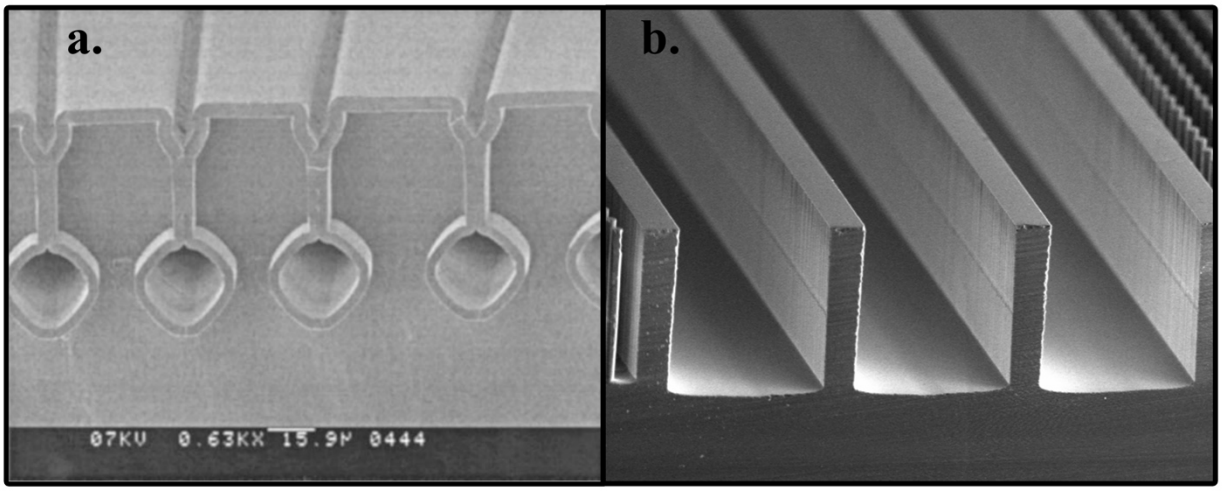

Figure 2.5: SEM images of (a) buried channel technology micro-machined channels, (b) open rectangular channels achieved through deep reactive ion etching. Copyright © 2000, IEEE

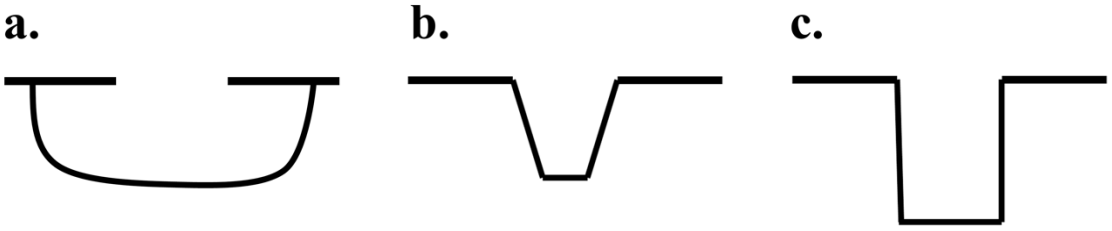

Figure 2.6: Cross-sectional view of different etch types. (a) isotropic etching, (b) anisotropic wet etching, (c) anisotropic dry etching.

an electrical current through the Pyrex and silicon wafers, a chemical bond is established due to the migration of free ions in the Pyrex [19]. To complete these columns, standard micro-capillaries are connected in order to interface them with the rest of the GC system.

2.5. Micro-Separation Columns

As to the actual design of these uSCs, there have been several introduced since their invention. Starting with the basic, there is the open rectangular column. Another variation of this design is the buried channel technology column [18]. These are similar to the wall coated open tubular separation columns of traditional GC in that they are functionalized by coating the walls of the channel with the stationary phase. And like the open tubular columns, they show very similar plate height numbers and behavior. However, since these MEMS-based columns are much shorter and can complete a similar separation in a significantly less amount of time [10,20].

In the years since, there have been several new designs introduced with an aim to increase the separation efficiency of uSCs. Some examples include changing the shape of the column from a double spiral to a serpentine [21], or even the shape of the channels themselves [22–25]. One design that will be focused on is the semi-packed column (SPC) [15]. This new uSC was developed in order to combat some of the downsides of using an open rectangular column as well as introduce benefits that were lacking previously. The major change in SPCs versus the open rectangular

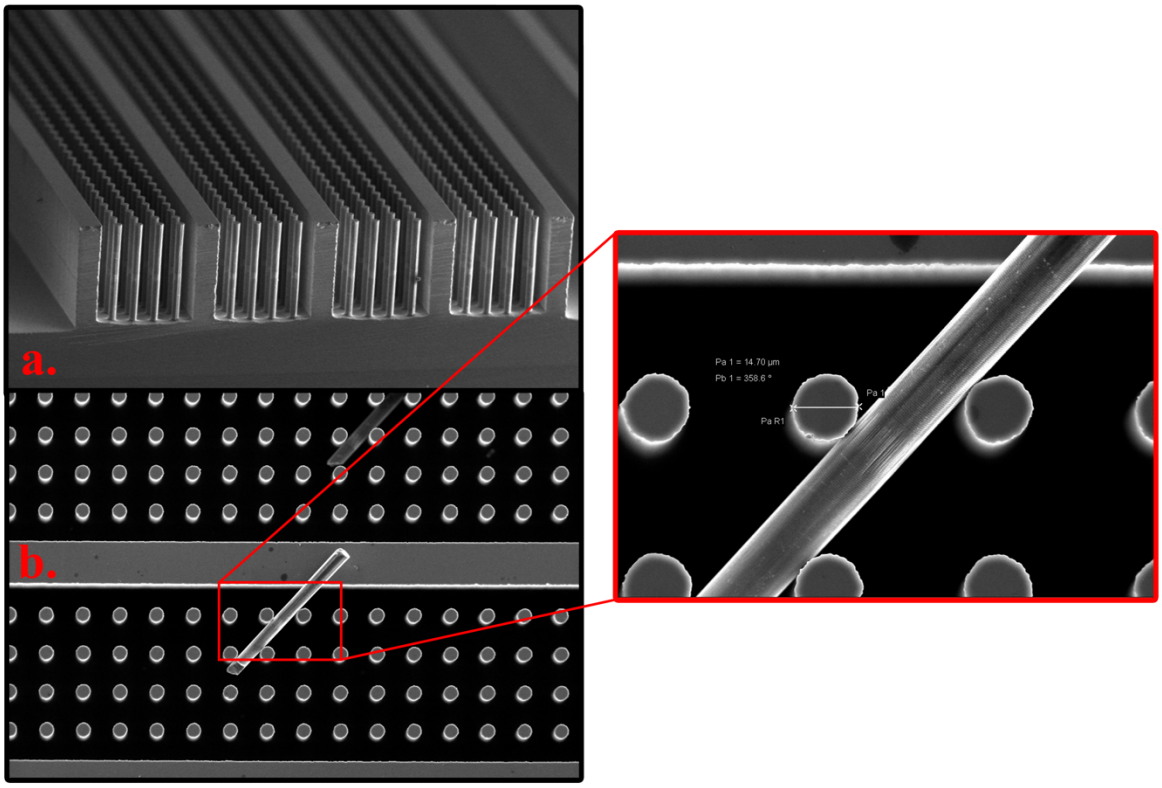

Figure 2.7: SEM images of a semi-packed column. (a) isometric view, (b) top-down view. Notice the pillar uniformity that is achieved due to the anisotropic etching. This can be seen clearly through the magnified view.

predecessor was in the inclusion of micro-pillars in the microfluidic channel as shown in Figure 2.7. The first benefit of including these micro-pillars was to increase the internal surface area of the column which subsequently allowed for a larger sample loading when compared to an open rectangular column. Second, this design allowed for a lower pressure drop and less band broadening due to eddy diffusion relatively when compared to packed columns in traditional GC. Lastly, by including the micro-pillars, the carrier gas velocity profile in the channel is more uniform and is exposed to shorter mass transfer distances [15]. Essentially, by including these micro-pillars in the channel, there is an increase in the separation efficiency due to a reduction of peak band broadening and a lower variation in the carrier gas velocity profile.

2.6. References

[1] L. R. Snyder, "Column efficiency in liquid-solid adsorption chromatography. H.E.T.P. [height equivalent to a theoretical plate] values as a function of separation conditions," *Anal. Chem.*, vol. 39, no. 7, pp. 698–704, Jun. 1967.

[2] W. L. Jones, "Modifications to the van Deemter Equation for the Height Equivalent to a Theoretical Plate in Gas Chromatography," *Anal. Chem.*, vol. 33, no. 7, pp. 829–832, Jun. 1961.

[3] H. M. McNair and E. J. Bonelli, "Basic gas chromatography," 1969.

[4] D. T. Sawyer, "Experimental gas chromatography (Miller, James M.)," *J. Chem. Educ.*, vol. 41, no. 3, p. A214, Mar. 1964.

[5] Poole Colin F. and Poole Salwa K., "Ionic liquid stationary phases for gas chromatography," *J. Sep. Sci.*, vol. 34, no. 8, pp. 888–900, Apr. 2011.

[6] D. W. Armstrong, L. He, and Y. S. Liu, "Examination of ionic liquids and their interaction with molecules, when used as stationary phases in gas chromatography," *Anal. Chem.*, vol. 71, no. 17, pp. 3873–3876, Sep. 1999.

[7] J. L. Anderson and D. W. Armstrong, "Immobilized Ionic Liquids as High-Selectivity/High-Temperature/High-Stability Gas Chromatography Stationary Phases," *Anal. Chem.*, vol. 77, no. 19, pp. 6453–6462, Oct. 2005.

[8] J. L. Anderson, J. Ding, T. Welton, and D. W. Armstrong, "Characterizing Ionic Liquids On the Basis of Multiple Solvation Interactions," *J. Am. Chem. Soc.*, vol. 124, no. 47, pp. 14247–14254, Nov. 2002.

[9] R. D. Rogers, "Materials science: Reflections on ionic liquids," *Nature*, vol. 447, no. 7147, pp. 917–918, Jun. 2007.

[10] S. C. Terry, J. H. Jerman, and J. B. Angell, "A gas chromatographic air analyzer fabricated on a silicon wafer," *IEEE Trans. Electron Devices*, vol. 26, no. 12, pp. 1880–1886, Dec. 1979.

[11] C.-J. Lu *et al.*, "First-generation hybrid MEMS gas chromatograph," *Lab. Chip*, vol. 5, no. 10, pp. 1123–1131, 2005.

[12] H. Kim *et al.*, "A Micropump-Driven High-Speed MEMS Gas Chromatography System," in *TRANSDUCERS 2007 - 2007 International Solid-State Sensors, Actuators and Microsystems Conference*, 2007, pp. 1505–1508.

[13] C.-Y. Kuo, P.-S. Chen, H.-T. Chen, C.-J. Lu, and W.-C. Tian, "Development of micromachined preconcentrators and gas chromatographic separation columns by an electroless gold plating technology," *J. Micromechanics Microengineering*, vol. 27, no. 3, p. 035012, 2017.

[14] B. Alfeeli, L. T. Taylor, and M. Agah, "Evaluation of Tenax TA thin films as adsorbent material for micro preconcentration applications," *Microchem. J.*, vol. 95, no. 2, pp. 259–267, Jul. 2010.

[15] S. Ali, M. Ashraf-Khorassani, L. T. Taylor, and M. Agah, "MEMS-based semi-packed gas chromatography columns," *Sens. Actuators B Chem.*, vol. 141, no. 1, pp. 309–315, Aug. 2009.

[16] M. Akbar, H. Shakeel, and M. Agah, "GC-on-chip: integrated column and photoionization detector," *Lab Chip*, vol. 15, no. 7, pp. 1748–1758, 2015.

[17] S. Nair and S. Narayanan, "MicroGC: Of Detectors and their Integration," Apr. 2014.

[18] M. J. de Boer *et al.*, "Micromachining of buried micro channels in silicon," *J. Microelectromechanical Syst.*, vol. 9, no. 1, pp. 94–103, Mar. 2000.
[19] M. Akaike and T. Yagi, *Anodic bonding process*. Google Patents, 1998.
[20] M. Agah, G. R. Lambertus, R. D. Sacks, and K. D. Wise, "High-speed MEMS-based gas chromatography," in *IEDM Technical Digest. IEEE International Electron Devices Meeting, 2004.*, 2004, pp. 27–30.
[21] A. D. Radadia, A. Salehi-Khojin, R. I. Masel, and M. A. Shannon, "The effect of microcolumn geometry on the performance of micro-gas chromatography columns for chip scale gas analyzers," *Sens. Actuators B Chem.*, vol. 150, no. 1, pp. 456–464, Sep. 2010.
[22] M. A. Zareian-Jahromi, M. Ashraf-Khorassani, L. T. Taylor, and M. Agah, "Design, Modeling, and Fabrication of MEMS-Based Multicapillary Gas Chromatographic Columns," *J. Microelectromechanical Syst.*, vol. 18, no. 1, pp. 28–37, Feb. 2009.
[23] H. Yuan *et al.*, "The effect of the channel curve on the performance of micromachined gas chromatography column," *Sens. Actuators B Chem.*, vol. 239, no. Supplement C, pp. 304–310, Feb. 2017.
[24] A. D. Radadia, R. I. Masel, and M. A. Shannon, "New Column Designs for MicroGC," in *TRANSDUCERS 2007 - 2007 International Solid-State Sensors, Actuators and Microsystems Conference*, 2007, pp. 2011–2014.
[25] H. Shakeel, D. Wang, J. R. Heflin, and M. Agah, "Width-Modulated Microfluidic Columns for Gas Separations," *IEEE Sens. J.*, vol. 14, no. 10, pp. 3352–3357, Oct. 2014.

3. Ionic liquid functionalization of semi-packed columns for high-performance gas chromatographic separations

(This chapter previously appeared as B. P. Regmi, R. Chan, and M. Agah, "Ionic liquid functionalization of semi-packed columns for high-performance gas chromatographic separations," Journal of Chromatography A. It is reproduced by permission of Elsevier. https://doi.org/10.1016/j.chroma.2017.06.050)

3.1. Abstract

Gas chromatography columns fabricated using microelectromechanical system (MEMS) technology provide a number of clear advantages. However, successful deposition of stationary phases having a wide application range remains an important technical challenge. In this paper, we report, for the first time, on the deposition of room temperature ionic liquids (RTILs)—a versatile class of stationary phases—inside the channels of semi-packed columns (SPCs) for high-performance gas chromatographic separation of complex chemical mixtures. A 1 m long, 240 µm deep, 190 µm wide column comprising an array circular micropillars of 20 µm in diameter and 40 µm post spacing was fabricated using MEMS processes. Two RTILs were immobilized inside these columns using a dynamic coating method, and the columns were tested for separation of three different mixtures: a 15-component mixture of hazardous chemical pollutants, an 8-component mixture of fatty acid methyl esters, and a sample of gasoline. These columns displayed sharp and symmetrical peaks, significant selectivity variation between the two columns, and rapid

separation times. The columns yielded high separation efficiencies measured by approximately 2300 plates/m under isothermal conditions. This work highlights the potential of RTILs to be used as excellent stationary phases for SPCs, thereby dramatically expanding the range of complex mixtures that could be analyzed using a micro gas chromatograph.

3.2. Introduction

Gas chromatography (GC) is a powerful analytical technique that has been widely used for the separation and analysis of individual components of complex mixtures comprising volatile or semi-volatile compounds. Given its widespread applications, the development of portable and miniaturized GC is an area of growing scientific interest. The heart of a GC system is the separation column which is crucial for overall performance of a chromatographic analysis. There has been intensive studies in the development of miniaturized separation columns [1-7], and in this regard micromachined silicon-glass chips have been a focus of several research studies [2-7]. These columns can consume low power (less than 100 mW) [8] and enable rapid temperature programming (up to 60 °C/s) [5]. Additionally, it is possible to make micro columns of desired shapes and geometrical patterns which are otherwise unobtainable in traditional GC columns. These micromachined silicon columns have been successfully integrated with other microfabricated components to develop portable gas chromatography systems in both research [9,10] and commercial laboratories [11,12]. Our group took significant effort to develop a new class of micro columns named as semi-packed columns (SPCs) which provide higher separation efficiencies and sample capacities compared to the open-channel counterparts [2,3,13]. These columns exhibit the properties of both packed columns—high sample capacity—and open tubular columns—high speed separation, high separation efficiency, and low pressure drop. These

columns have already garnered substantial attention from other research groups [14-18]. In contrast to open channel columns, the SPCs exhibit smaller loss of efficiency with the increase in flow rate [17,18], thereby making them suitable for high speed separations.

The stationary phase coated inside microfabricated channels plays a central role in the separation process, and there have been considerable efforts to develop new stationary phase materials for micro columns (μCs). Several reports have been recently published on the use of monolayer-protected gold [19-21], carbon nanotubes [5,22], polymers [18,23,24], metal-organic frameworks [25], atomic layer-deposited alumina [26,27], sputtered oxides or graphite [14,28,29], and silica nanoparticles [30] as stationary phases in μCs. Despite these encouraging studies, there is still a need to overcome a number of limitations and critical points. First, a considerable band broadening and/or tailing has been observed leading to a loss in separation power [11,18,23]. Second, some of these microfabircated columns show limited chemical selectivity—although they show promising separation performance—thereby confining their applications [26,29]. It is therefore desirable to develop and evaluate new stationary phases that can overcome the aforementioned limitations. Among a number of different stationary phase materials, one promising class of compounds that await full exploration in microfluidic columns is ionic liquids (ILs).

ILs constitute a group of organic salts which are liquid below 100 °C; and the ILs that are liquid at room temperature are commonly known as room temperature ionic liquids (RTILs) [31]. ILs are polar, chemically inert, nonflammable, thermally stable, easy to synthesize, possess low vapor pressure, and their selectivity can be easily tuned by altering the constituent cation or anion; and hence they have been widely used as stationary phases in conventional gas chromatography

[32-38]. Currently, more than 300 ILs are commercially available and more than a trillion ILs have been estimated [39,40]. Remarkably, RTILs can separate both polar and non-polar analytes [33]. They have abilities to undergo multiple solvent-solute interactions which include: nonbonding and π-electron interactions, dipole-type interactions, hydrogen bonding (basicity and acidity) interactions, and cohesion and dispersion interactions [41]. ILs show significant hydrogen bond acidity, a feature that is absent in commonly used conventional stationary phases, such as poly(siloxane) and poly(ethylene glycol) [42]. Unlike conventional stationary phases which provide limited selectivity variations, ILs offer excellent opportunities for fine-tuning the selectivity of the stationary phase. They have also been increasingly used in multidimensional and high speed GC [43-45]. Although ILs have been extensively utilized as stationary phases in open tubular and packed columns [42], the separation performance of ILs in MEMS-based columns have not studied yet except for a published work by Zellers and coworkers [46]. The authors attempted to use an RTIL-coated open rectangular column as a second dimension column in a 2-dimensional GC. The micro column produced reasonably good peak shapes; however, excessively broad peaks were obtained with polar compounds that led to low ^{2}D resolution. The authors attributed this excessive band broadening to localized pooling of the RTIL on the walls of the micro column.

Herein, we report, for the first time, the successful integration of SPCs with RTILs for high performance separation of complex chemical mixtures. To achieve this goal, we selected two RTILs, namely, trihexyltetradecylphosphonium bis(trifluoromethylsulfonyl)imide ([P66614][NTf2]) and 1-butylpyridinum bis(trifluoromethylsulfonyl)imide ([BPyr][NTf2]) as stationary phases. These RTILs were immobilized inside SPCs using a dynamic coating method. The performance of these columns was evaluated by separating a number of chemical mixtures,

including a 15-component mixture of hazardous chemical pollutants, an 8-component mixture of fatty acid methyl esters (FAMEs), and a sample of gasoline. These RTIL-coated columns exhibited sharp and symmetrical peaks, rapid separation times, and high separation efficiency of approximately 2300 plates/m. The tailing factor of the peaks was found to be between 0.92 and 1.76. The selectivity of the two columns were found to be substantially different. Given the fact that the selectivity of RTILs can be easily tuned by altering the constituent ions, these studies will open up new avenues to develop high-performance micro columns for the separation of a wide range of complex chemical mixtures.

3.3. Materials and methods

3.3.1. Materials

Silicon wafers were obtained from University Wafers. Borofloat wafers were purchased from Coresix Precision Glass, Inc. Fused silica capillary tubes of 100 μm internal diameter and 200 μm outer diameter were obtained from Polymicro Technologies. A two-part epoxy system was obtained from J-B Weld. Acetone was obtained from Spectrum Chemicals. Hexane, heptane, benzene, toluene, ethylbenzene, p-xylene, m-xylene, o-xylene, styrene, benzyl chloride, 1,2-dichlorobenzene, 1,2,4-trichlorobenzene, naphthalene, 2-nitrotoluene, 3-nitrotoluene, and 4-nitrotoluene were obtained from Sigma Aldrich. A mixture containing 8 fatty acid methyl esters (FAME #20 mix) was obtained from Restek Corporation. Gasoline (octane rating of 87) was obtained from local Kroger Fuel Center. Air and ultrapure helium were purchased from Airgas, Inc. Methane was obtained from Air Liquide, Inc. Ultrapure hydrogen for flame ionization detector

(FID) was produced by using Parker Domnick Hunter hydrogen generator All of these chemicals were used as received without further purification.

3.3.2. Column Fabrication

The separation columns were produced employing microelectromechanical system (MEMS) processes including photolithography, etching, and silicon-glass anodic bonding. The configuration of the columns was serpentine. The fabricated columns were 1-meter long, 240 μm deep and 190 μm wide with circular pillars of 20 μm diameter and 40 μm pillar spacing. The fabrication procedure was similar to our previously reported work [3]. A silicon wafer was cleaned using standard RCA cleaning, and then it was primed with hexamethyldisilazane (HMDS) which acts as an adhesion promotor for a photoresist. This is followed by the deposition of 8 μm thick AZ9260 photoresist by spin coating at 2000 rpm for 1 minute. The photoresist-coated wafer was then soft-baked at 110 °C for 1 minute. The pattern from a chrome mask was transferred to the soft-baked wafer by using ultra violet light source and a mask aligner. The wafer was then hard-baked at 110 °C for 3 minutes. Following this, the wafer was anisotropically etched using Alcatel deep reactive ion etcher (DRIE) via a standard Bosch process with SF_6 as etching and C_4F_8 passivation reactants. The photoresist was removed by treating the wafer with acetone and subsequently with piranha solution. The etched silicon wafer was anodically bonded with a 700 μm thick Borofloat wafer (Coresix Precision Glass) at 1250 V and 400 °C for 45 minutes, and finally the wafer was diced into individual devices. The outlet and inlet of the column were then connected to fused silica capillary tubing (internal diameter: 100 μm and outer diameter: 200 μm) using J-B Weld twin tube epoxy in order to connect the micro column to GC injection port and detector. The total length of the two capillary tubes was 27 cm.

3.3.3. Column Coating

A freshly prepared solution of an RTIL in acetone at a concentration of 8 mg/mL (for dynamic) and 2 mg/mL (for static) was used for deposition of RTILs into the channels of the SPCs. Both static and dynamic coating methods were explored. Static coating did not produce high yields for SPCs since air bubbles were formed during the coating procedure preventing the deposition of the RTILs in some of these columns. Therefore, we selected the columns coated with the dynamic technique for our chromatographic evaluation of RTIL-functionalized SPCs.

3.3.4. Data acquisition

The separations were performed using an Agilent 7890A GC system equipped with an automatic sampler (7693A) and two FIDs. The schematic diagram of the measurement setup is shown in **Figure 1**. Helium was used as a carrier gas. Before installation, the columns were flushed with nitrogen for 30 minutes. Following the installation, each column was conditioned from 30 to 200 °C at a ramp rate of 2 °C/min followed by holding at 200 °C for 15 minutes, while the inlet pressure was held at 10 psi during the column conditioning. The inlet temperature was kept at 280 °C and the detector temperatures was kept at 300 °C during the measurements. Data collection and analysis was performed using Agilent ChemStation Edition C.01.04.

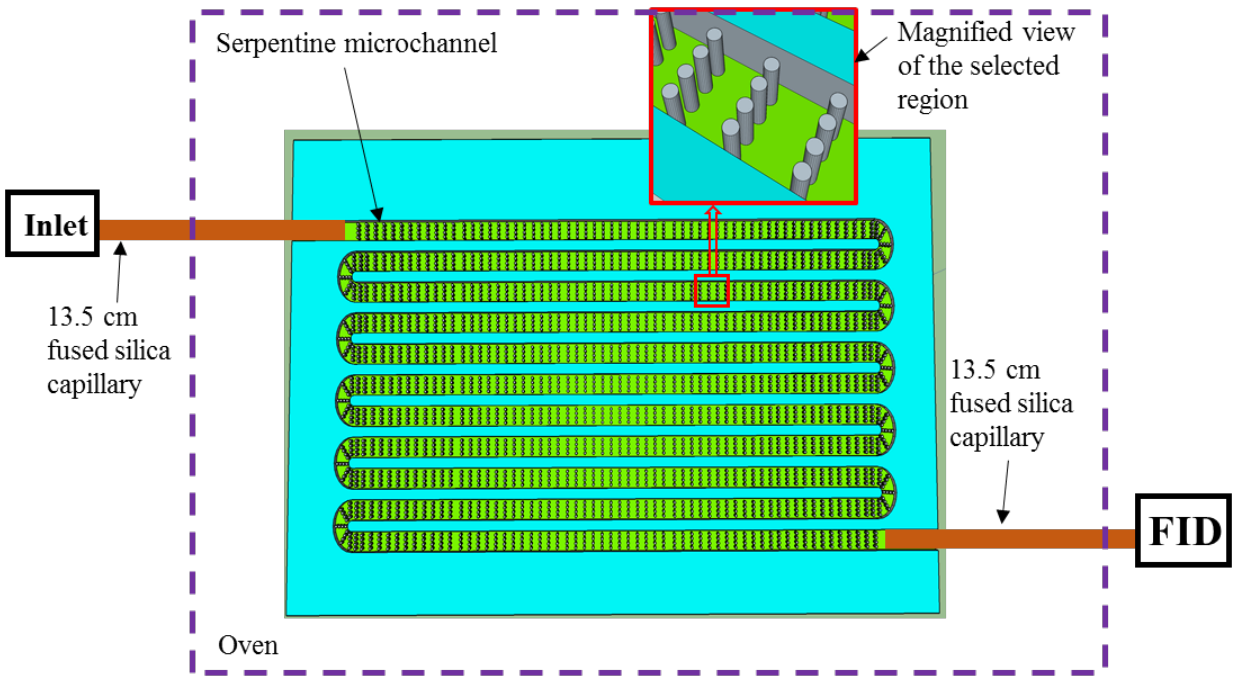

Figure 3.1: Schematic diagram of the measurement setup.

3.4. Results and Discussion

3.4.1. Selection of RTILs

We selected [P66614][NTf2] and [BPyr][NTf2] as the model RTILs since they are expected to show altered selectivity due to the presence of distinctly different cations. Among these two RTILs, [P66614][NTf2] has been previously used as a GC stationary phase and it has been shown to be stable up to 380 °C [38]. To the best of our knowledge, the RTIL [BPyr][NTf2], however, has not been used as a stationary phase in GCs. In order to evaluate the thermal stability, we followed the procedure established in [32]. We coated a thin film of [BPyr][NTf2] inside a fused silica capillary tubing. Then the coated capillary was heated in the GC oven. The temperature was

ramped from 30 to 320 °C at a rate of 10 °C/min. FID signal during this time did not show any significant rise in its baseline indicating that the RTIL is stable at least up to 320 °C, which is sufficient for the separation of a wide range of analytes.

3.4.2. Characterization of the coated columns

The coated SPCs were imaged using an optical microscope. **Figures 3.2a-c** show the optical images of a portion of the uncoated and coated columns. The dynamic coated columns show some isolated microdroplets of varying sizes, indicating that the RTIL deposits were not continuous. These observations are consistent to the previous reports that RTIL coatings exhibit particulate topology [47,48].

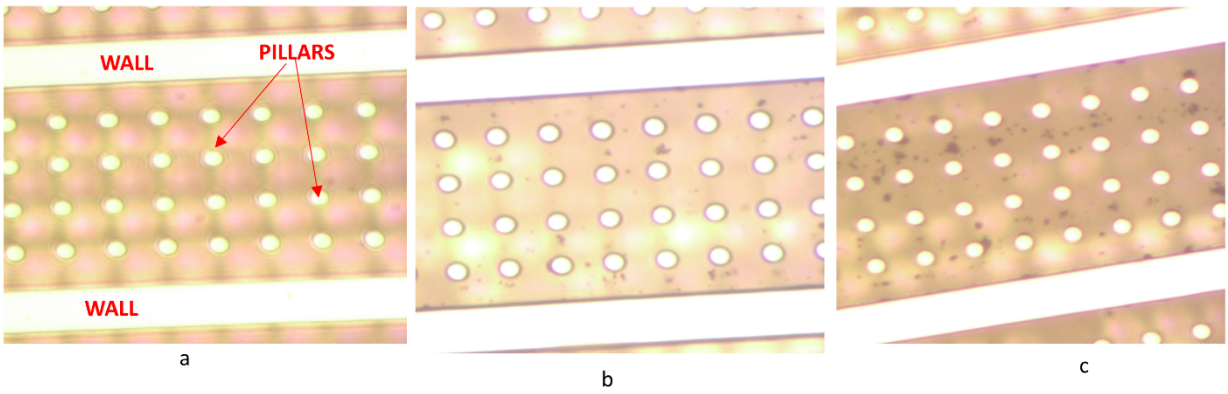

Figure 3.2: Optical micrographs of SPCs: a) uncoated, b) coated with [P66614][NTf2], and c) coated with [BPyr][NTf2].

3.4.3. Evaluation of separation efficiency

The separation efficiency of each column was evaluated by determining the height-equivalent-to-a-theoretical plate (HETP) as a function of the average carrier gas linear velocity. The retention

time of methane was taken as the hold-up time. HETP were determined at 100 °C isothermal conditions using naphthalene as a probe. The following equations were used for calculations.

$$\bar{u} = \frac{L}{t_{\mathrm{M}}} \quad (1) \qquad k = \frac{t_{\mathrm{R}} - t_M}{t_{\mathrm{M}}} \quad (2) \qquad N = 5.545 \left(\frac{t_R}{w_{\mathrm{h}}}\right)^2 \quad (3) \qquad H = \frac{L}{N} \quad (4)$$

where, $\bar{u}$ is average linear velocity, L is the length of a column, t_{M} is the retention time of methane, t_{R} is the retention time of the compound of interest, N is the number of theoretical plates, w_{h} is the peak width at half height of the compound of interest, and H is HETP.

Figure 3.3 shows the Golay plots (H vs $\bar{u}$) for the columns coated with the two RTILs. The minimum plate height for the [P66614][NTf2]-coated column was found to be 0.047 cm (maximum number of theoretical plates of 2128 plates per meter) at a flow rate of 24 cm/sec (k for naphthalene = 14.5). Similarly, the minimum plate height for the [BPyr][NTf2]-coated column was found to be 0.044 cm (maximum number of theoretical plates of 2273 plates per meter) at a flow rate of 23 cm/s (k for naphthalene = 8.5). As evident from the Golay plots, the loss of efficiency was not very substantial as the flow rate increases. Efforts to optimize the coating to further enhance the separation efficiency are currently underway in our lab.

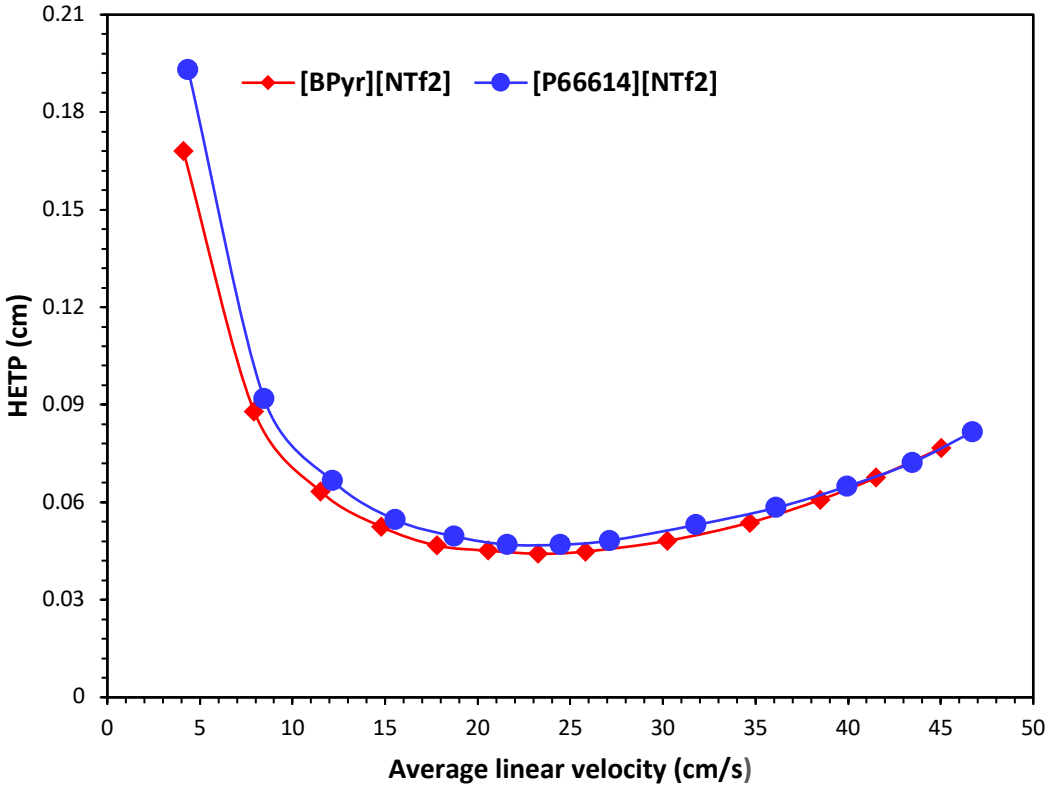

Figure 3.3: Variation of HETP as a function of the average velocity of the carrier gas (helium) for columns coated with two different RTILs. The HETP was determined using naphthalene as a probe under isothermal conditions. Chromatographic conditions for each column: injection volume 0.1 µL (2% naphthalene in heptane), split ratio 100:1, inlet temperature 280 °C, detector temperature 300 °C, and the oven temperature 100. The inlet pressure was varied from 2.5 to 45 psi. The legend shows the RTIL deposited in each column.

3.4.4. Mixture separation

The separation performance of the columns was characterized by separating a number of different mixtures. The first test mixture was a 15-component mixture comprising hydrocarbons, aromatic halides, and nitroaromatic compounds. These compounds include heptane, benzene, toluene, ethylbenzene, p-xylene, m-xylene, o-xylene, styrene, benzyl chloride, 1,2-dichlorobenzene, 1,2,4-trichlorobenzene, naphthalene, 2-nitrotoluene, 3-nitrotoluene, and 4-nitrotoluene. The boiling points of these compounds range from 80.1 to 238 °C. These toxic chemicals are widely distributed in environmental and occupational settings, and there has been

substantial scientific interest in monitoring these chemicals. **Figure 3.4a-b** show chromatograms for the separation of this mixture. These chromatograms were obtained under temperature and pressure programmed conditions. It is evident from these chromatograms that these compounds are well-resolved (except p- and m-xylenes), the peaks are sharp and symmetrical, and the separation is very rapid. Notably, the change in cation produced a considerable effect on separation selectivity as evident by the substantial changes in the relative retention. A change in elution order of some compounds is observed. In order to check the reproducibility, we coated two different columns with two different solutions of [BPyr][NTf2], the difference in retention times and number of theoretical plates for this set of analytes was less than 10% (data not shown).

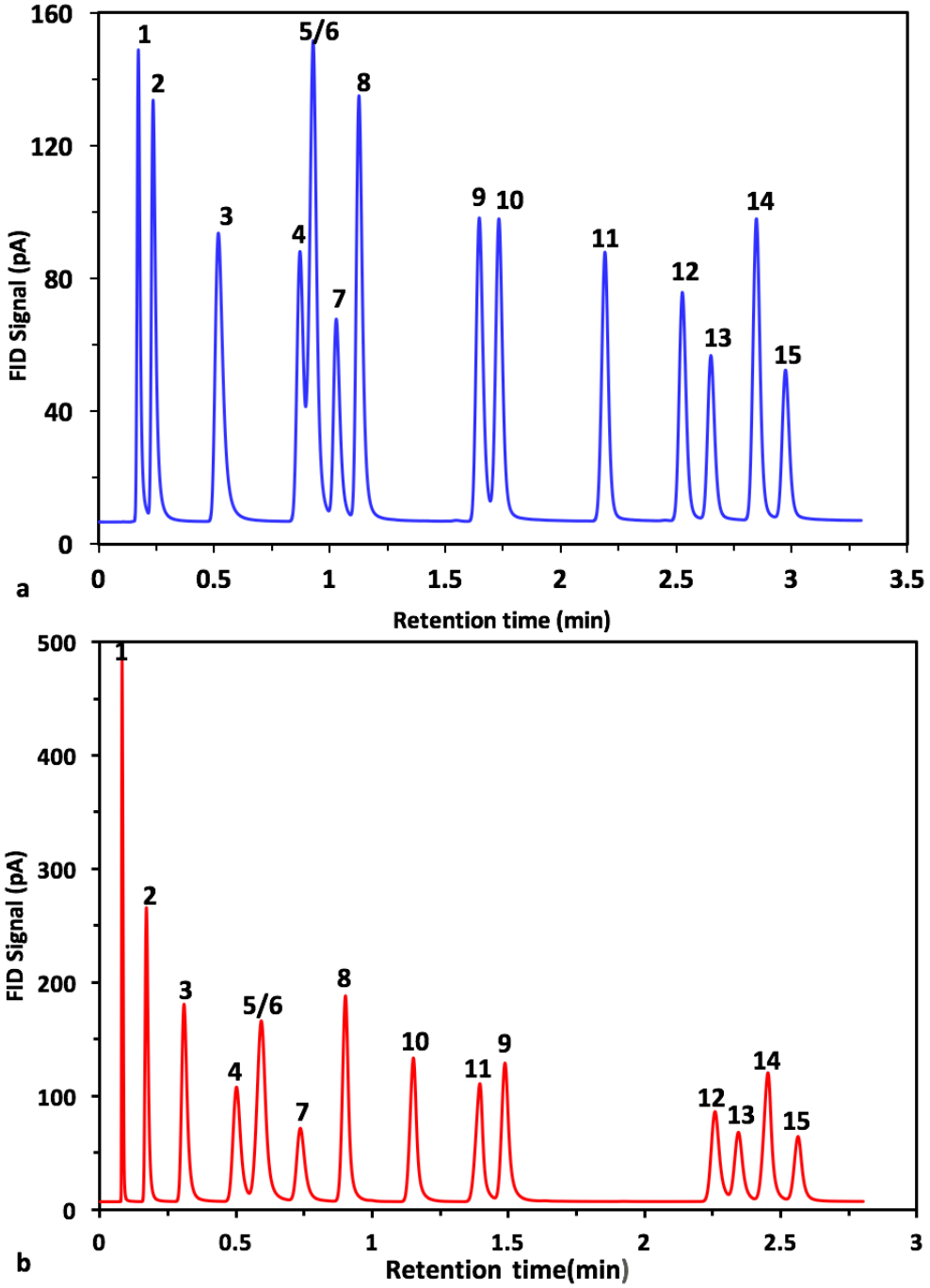

Figure 3.4: Separation of 15-compound mixture using a) [P66614][NTf2]- and b) [BPyr][NTf2]-coated columns. Chromatographic conditions: injection volume 0.1 µL, split ratio 400: 1, inlet pressure 17.5 psi for 0.8 min and then ramped to 25 psi at the rate of 60 psi/min, oven temperature 30 °C for 0.3 min and then ramped at the rate of 40 °C/min to 150 °C (for a) or 130 °C (for b). Peak identification: (1) heptane, (2) benzene, (3) toluene, (4) ethylbenzene, (5/6) p- and m-xylenes, (7) o-xylene, (8) styrene, (9) benzyl chloride, (10) 1,2-dichlorobenzene, (11) 1,2,4-trichlorobenzene, (12) naphthalene, (13) 2-nitrotoluene, (14) 3-nitrotoluene, and (14) 4-nitrotoluene.

The peak symmetry was evaluated by calculating the symmetry factor (or tailing factor), A_s, which is defined as:

$$A_s = \frac{W_{0.05}}{2f} \qquad (5)$$

where, $W_{0.05}$ is the width of the peak at 5% height and f is the distance from the peak maximum to the leading edge of the peak measured at 5% of the peak height. The tailing factor was found to be between 1.09 and 1.76 (Table S1, Supplementary Data). Tailing factors between 0.9 and 1.2 are acceptable, and tailing factors up to 2 may be acceptable depending on the resolution and separation; however tailing factor more than 2.0 requires to fix the problem [49].

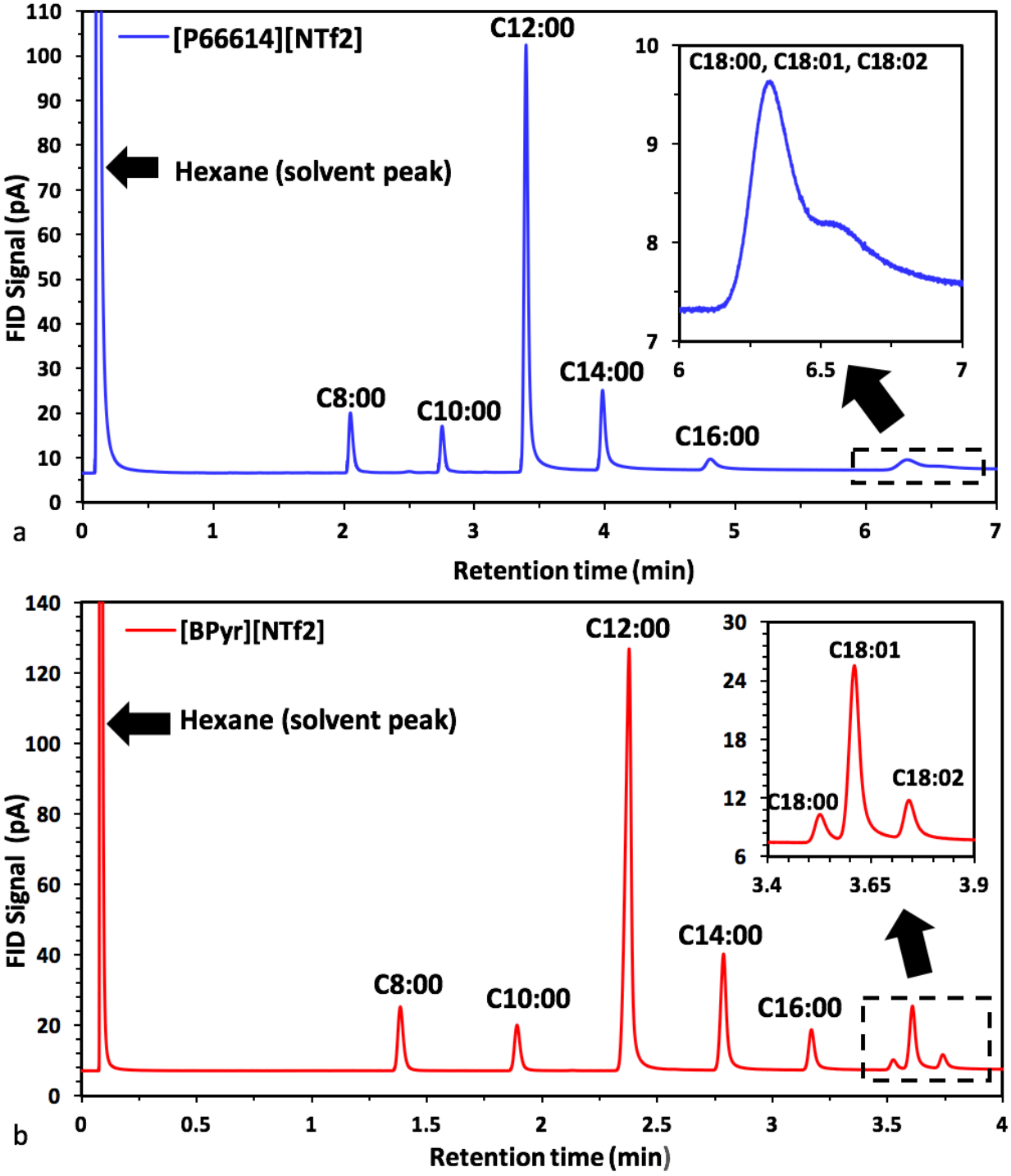

Figure 3.5: Separation of a mixture of 8 fatty acid methyl esters using a) [P66614][NTf2]- and b)[BPyr][NTf2]-coated columns. The identity of each peak is labeled. Insets show the magnified view of the selected regions. Chromatographic conditions: injection volume 0.1 µL, split ratio 100: 1, inlet pressure 17.5 psi for 0.8 min and then ramped to 25 psi at the rate of 60 psi/min, oven temperature 30 °C for 0.3 min and then ramped at the rate of 40 °C/min to 170 °C and held at 170 °C. The mixture of fatty acid methyl esters was dissolved in hexane at a concentration of 50 mg/mL.

Another group of analytes was a standard mixture containing 8 fatty acid methyl esters (FAMEs) obtained from Restek Corpotation. Analysis of FAMEs is very important for food and biodiesel characterization. The different FAMEs present in our test mixture were methyl caprylate (C8:00), methyl caprate (C10:00), methyl laurate (C12:00), methyl myristate (C14:00), methyl palmitate (C16:00), methyl stearate (C18:00), methyl oleate (C18:01), and methyl linoleate (C18:02). The mixture was dissolved in hexane (50 mg of total FAMEs was dissolved in 1 mL hexane). **Figure 3.5a** shows that [P66614][NTf2]-coated column could not separate C18:00, C18:01, and C18:02, while other FAMEs were baseline separated. Interestingly, as shown in **Fig. 3.5b**, [BPyr][NTf2]-coated column was able to baseline separate all these 8 compounds in less than 4 minutes. A decrease in the amount of each FAME by 10 times still showed clearly separated peaks (**Fig. S1**, Appendix A) and an increase in the amount by 5 times showed baseline separated peaks, except C18:00 and C18.01 which were almost baseline separated (**Fig. S2**, Appendix A). The tailing factor for different compounds were found to be between 0.92 and 1.76 (Table S2, Appendix A)

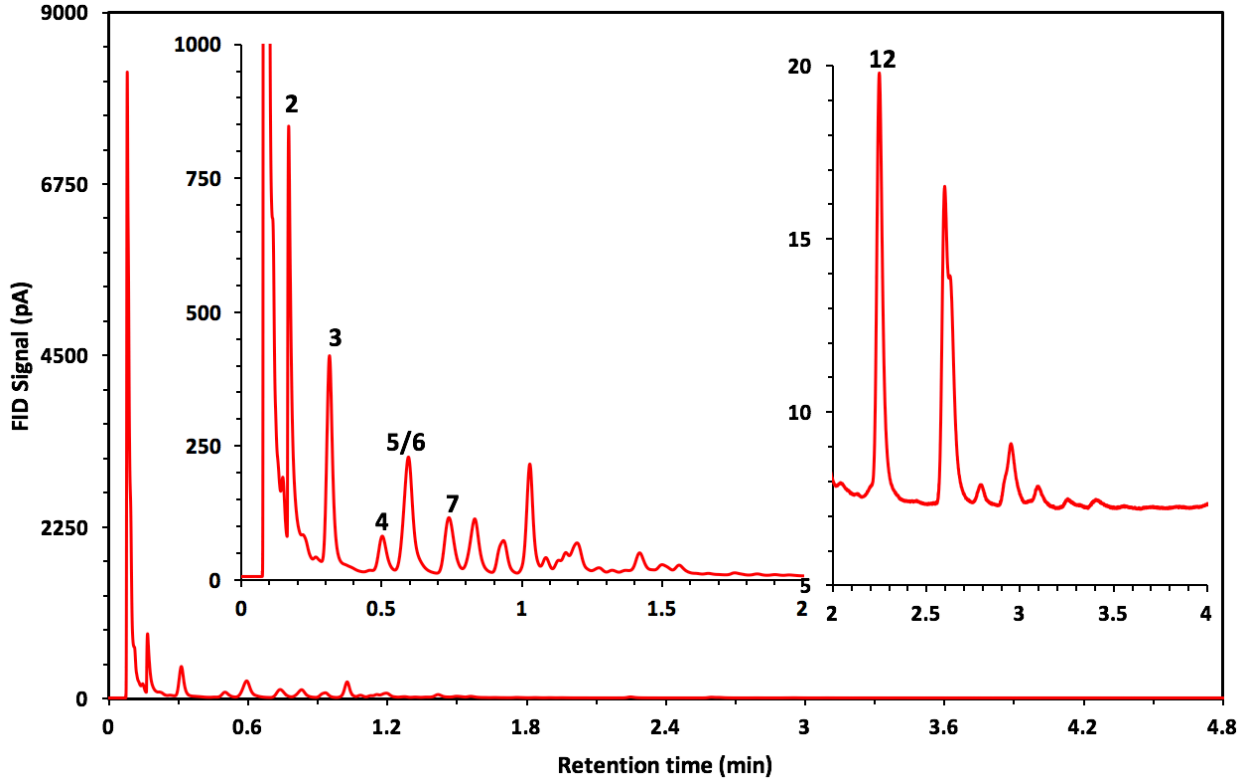

Figure 3.6: Separation of neat gasoline sample using a [BPyr]][NTf2]-coated column. Chromatographic conditions: injection volume 0.1 µL, split ratio 100: 1, inlet pressure 17.5 psi for 0.8 min and then ramped at the rate of 60 psi/min to 25 psi and hold at the pressure, oven temperature 30 °C for 0.3 min and then ramped at the rate of 40 °C/min to 170 °C and hold at 170 °C for 1 min. Insets show the magnified view of selected regions. The numbered peaks are those whose retention times match with the known compounds shown in Fig. 3.4.

The third mixture was a sample of gasoline. Automotive gasoline is a complex mixture of mostly low-boiling hydrocarbons, but it also contains hazardous chemicals such as BTEX (benzene, toluene, ethylbenzene, and xylenes) and naphthalene. The separation and determination of BTEX, naphthalene, and other hazardous chemical entities in gasoline and gasoline-contaminated environmental samples is crucial for efficient health risk assessment and management of occupational and environmental exposure to these chemicals. **Figure 6** shows the chromatogram for the separation of neat gasoline sample using [BPyr][NTf2]-coated column. It shows that the major fraction is low-boiling hydrocarbons which elute first. In addition, there are

a number of well separated peaks. **Figure 7** shows an overlay of chromatograms for gasoline and 15-component standard mixture obtained by using [BPyr][NTf2]-coated column. By matching the retention times, we can clearly see well resolved peaks of BTEX and naphthalene. The gasoline was also separated by using [P66614][NTf2]-coated columns (**Fig. S3,** Appendix A). Overlaying of chromatograms (**Fig. S4**, Appendix A) shows that some of the peaks of BTEX were not well resolved using this stationary phase.

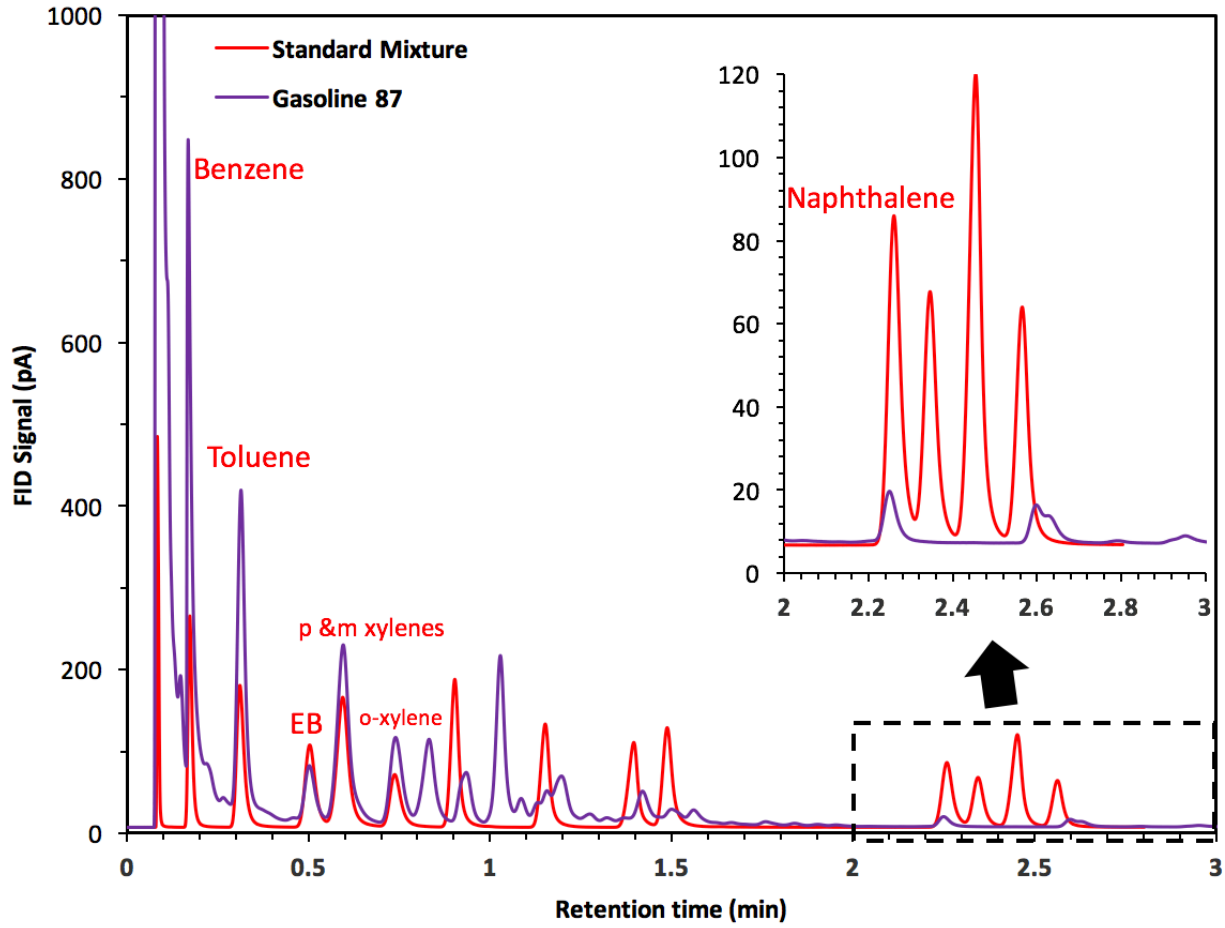

Figure 3.7: Overlay of chromatograms for the separation of gasoline (purple) and 15-component standard mixture (red) using a [BPyr][NTf2]-coated column. Inset shows the magnified view of the selected region. The peaks with retention time match are labeled.

Overall, these improved columns provide a series of advantages over the currently available micro columns. The first advantage is that these columns provide very sharp and symmetrical peaks. A careful examination of chromatograms of the earlier works or the commercially available micro columns shows that there is a significant peak broadening, fronting, or tailing [11,18,23] These effects arise due to either pooling of stationary phase at the corners of the rectangular columns or limited sample capacity of the columns [7]. Given the fact that we achieved symmetrical peaks for a number of polar and non-polar compounds, we presume that there is less pooling effects in the case of RTILs. Because of the outstanding characteristics of RTILs as a GC stationary phase, Collin et al. [46] attempted to immobilize an RTIL inside sodium chloride pretreated open rectangular micro column. However, this resulted excessive peak broadening for polar compounds, like 1,4-dioxane. This peak broadening was attributed to extreme retention of polar compounds due to localized pooling of the RTIL on the walls of the columns. However, we were able to immobilize the RTILs without having to pretreat the columns with sodium chloride although this pretreatment may enhance the separation performance. We presume that the presence of pillars may partially prevent the pooling of the RTILs inside the column. A highly polar compound, acetone, was passed through a column coated with [BPyr][NTf2], and as evident from **Fig. 8**, the peak is sharp (N= 2121 per meter) , although a slight tailing was observed. Note that approximately 200 ng of acetone was injected to obtain the chromatogram shown in **Fig. 8**, and no column overloading was noticed.

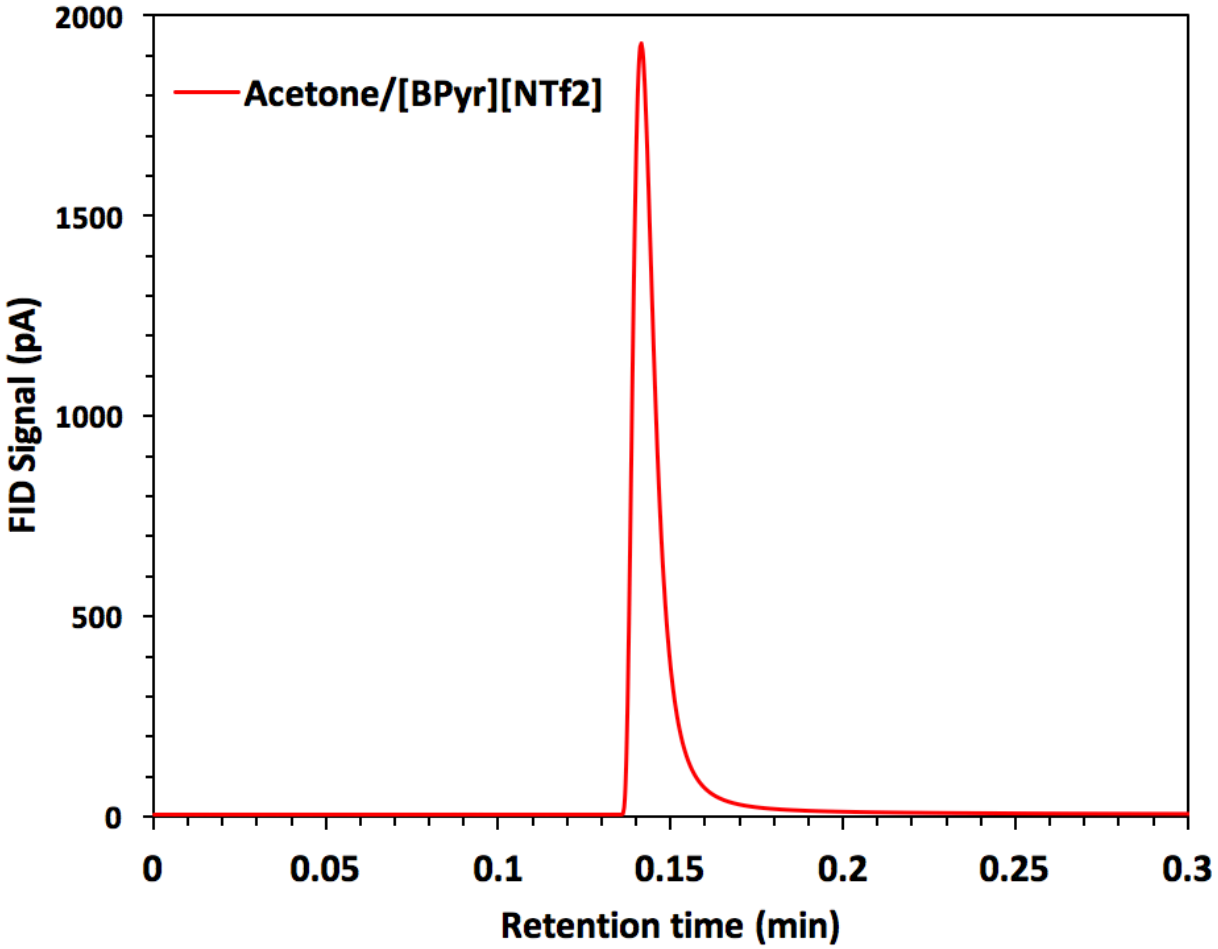

Figure 3.8: Acetone peak obtained at 50 °C under inlet pressure of 20 psi. Injection volume was 0.1 µL with a split ratio of 400:1. Number of theoretical plates is 2121 per meter.

The second advantage of this research is that it provides a route to create micro columns having different selectivity for separation of a wide range of chemical mixtures. Changing or modifying the constituent ions of an IL will modify the solvation properties of an IL, thereby altering the relative retention times. Although researchers are successful in the development of micro columns for high speed and highly efficient separation by using stationary phases, such as sputtered silica or graphite [29] and atomic layer deposited alumina [3,26], these stationary do not offer tunable

selectivity. The third advantage offered by these columns is the speed of separation. As discussed above, SPCs provide high efficiency and flatter Golay plots. It is therefore possible to work at higher flow rates to increase the separation speed without a significant loss in separation efficiency.

3.5. Conclusions

In this research, we successfully deposited two RTILs into the channels of microfarbicated SPCs using the dynamic coating method. These columns were used to separate a number of different chemical mixtures comprising both polar and non-polar compounds. These RTIL-coated SPCs displayed sharp and symmetrical peaks, offered high separation efficiency, and increased the separation speed. The number of theoretical plates obtained using helium as a carrier gas was as high as 2300 plate per meter, and the tailing factor of the peaks ranged from 0.92 to 1.76. The [BPyr][NTf2]-coated column showed promise for separation of BTEX and naphthalene from a sample of gasoline. Given the vast number of RTILs that could be employed for coating, these findings should broaden the applicability of the semi-packed GC columns for the analysis of a broad range of complex mixtures in different disciplines. Work is currently underway to optimize the coating procedure so as to achieve more uniform films which should further enhance the separation performance.

3.6. Appendix A

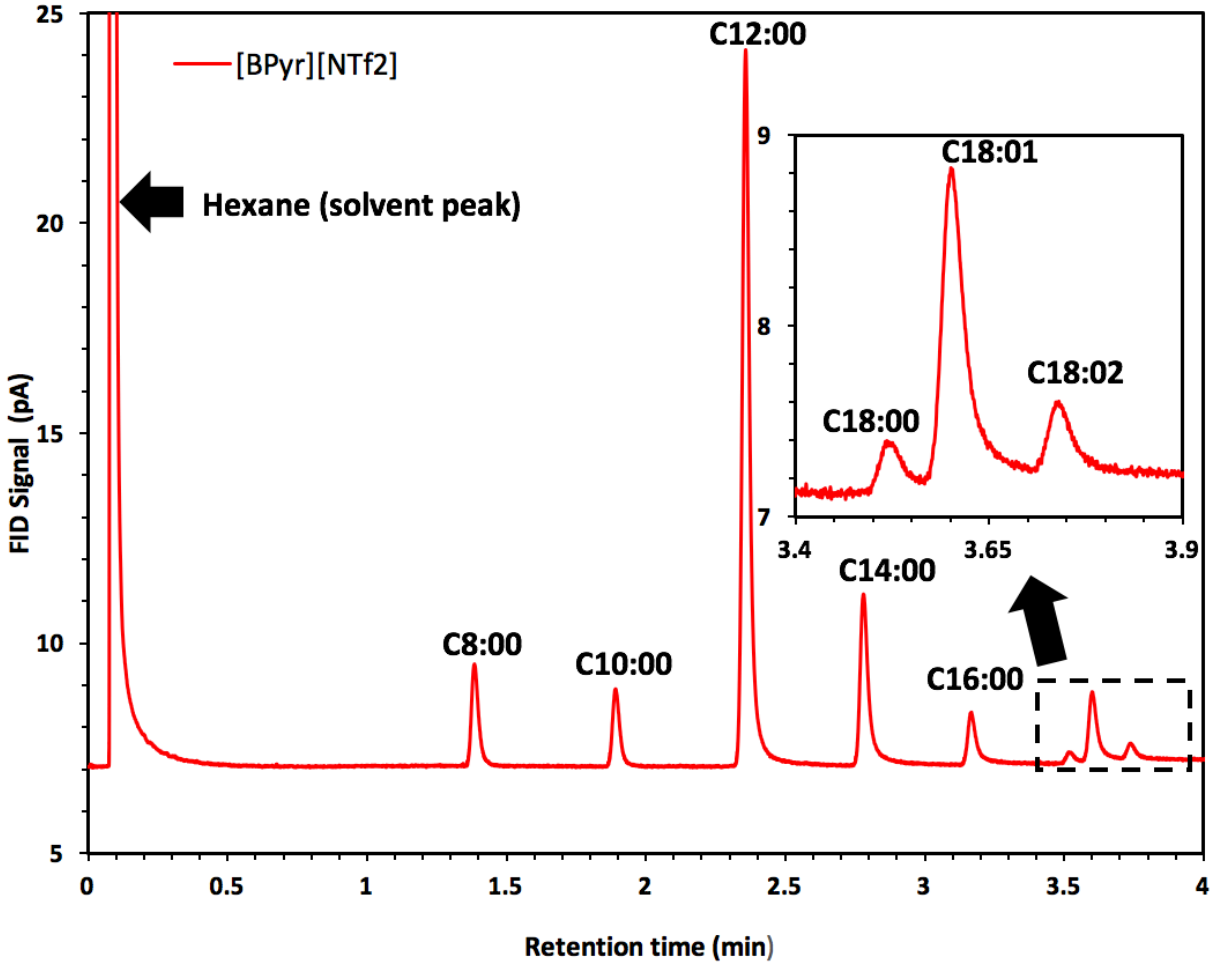

Figure S 1: Separation of a mixture containing 8 fatty acid methyl esters using a [BPyr][NTf2]-coated column. The identity of each peak is labeled. Inset shows the magnified view of the selected region. Chromatographic conditions: injection volume 0.1 µL, split ratio 100: 1, inlet pressure 17.5 psi for 0.8 min and then ramped to 25 psi at the rate of 60 psi/min, oven temperature 30 °C for 0.3 min and then ramped at the rate of 40 °C/min to 170 °C and held at 170 °C for 0.2 min. The mixture of fatty acid methyl esters was dissolved in hexane at a concentration of 5 mg/mL. The calculated amount of the different components entering the column is: 0.35 ng of C8:00, 0.25 ng of C10:00, 2.40 ng of C12:00, 0.75 ng of C14:00, 0.35 ng of C16:00, 0.15 ng of C18:00, 0.60 ng of C18:01, and 0.15 ng of C18:02.

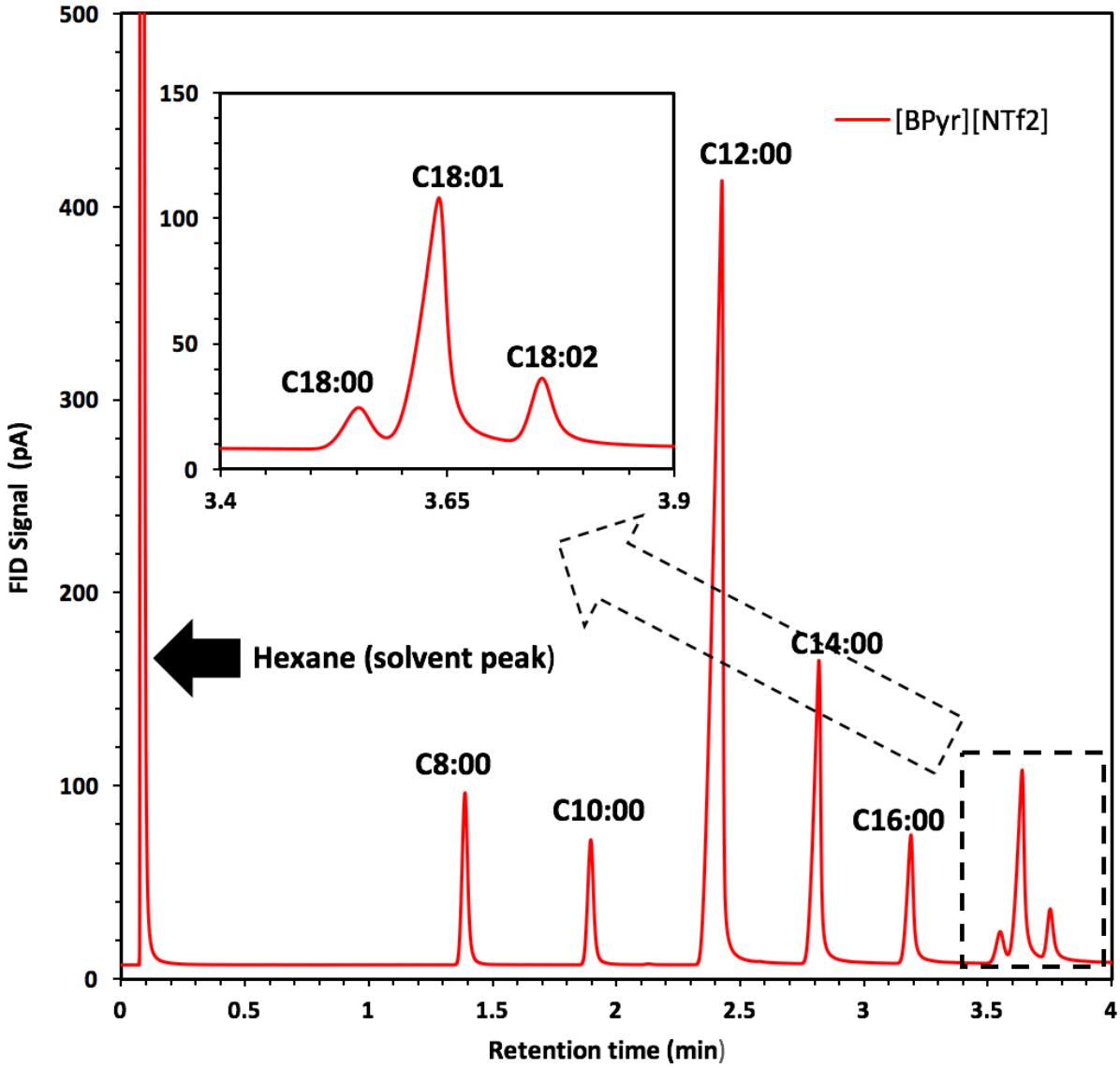

Figure S 2: Same as in Fig. S1 except that the injection volume was 0.5 µL of 50 mg/mL i.e., the amount of each compound entering the column was 50 times higher than that in Fig. S1.

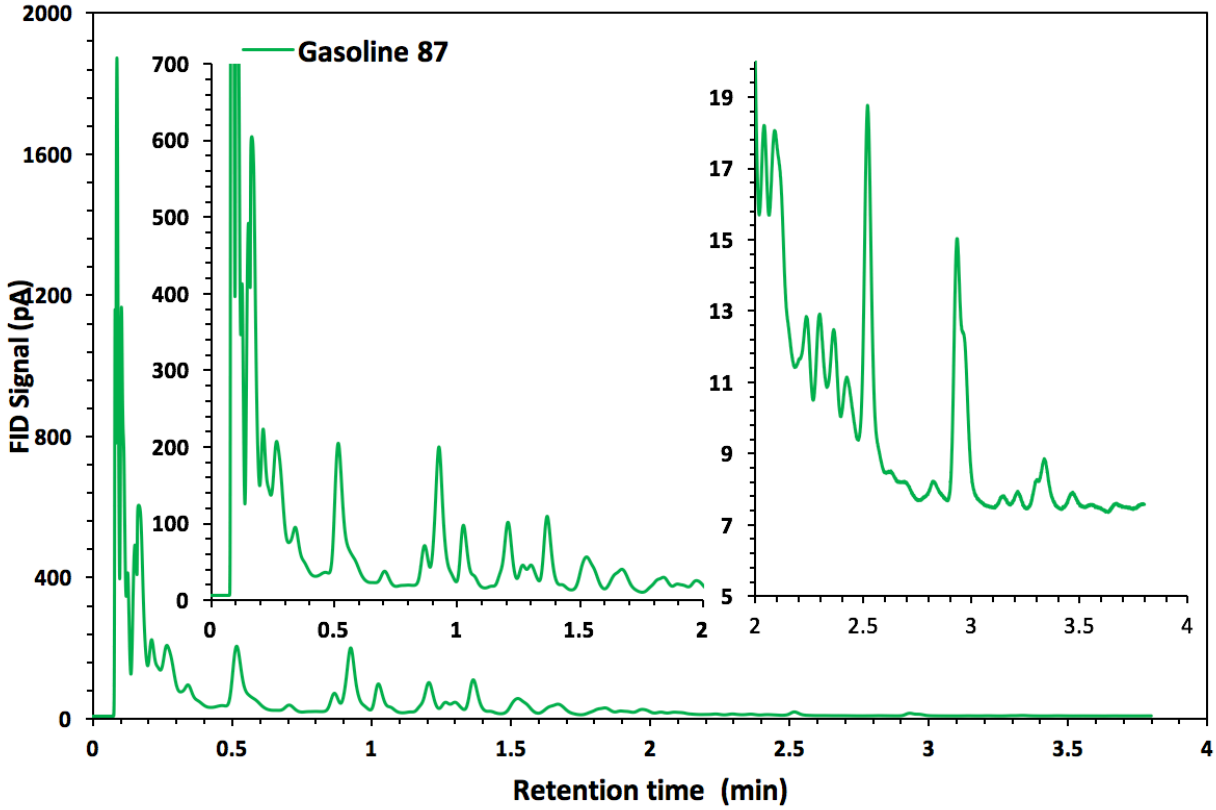

Figure S 3: Separation of neat gasoline sample using a [P66614]][NTf2]-coated column. Chromatographic conditions: injection volume 0.1 µL, split ratio 100: 1, inlet pressure 17.5 psi for 0.8 min and then ramped at the rate of 60 psi/min to 25 psi and held at the pressure, oven temperature 30 °C for 0.3 min and then ramped at the rate of 40 °C/min to 170 °C and held at 170 °C for 1 min. Insets show the magnified view of the selected regions.

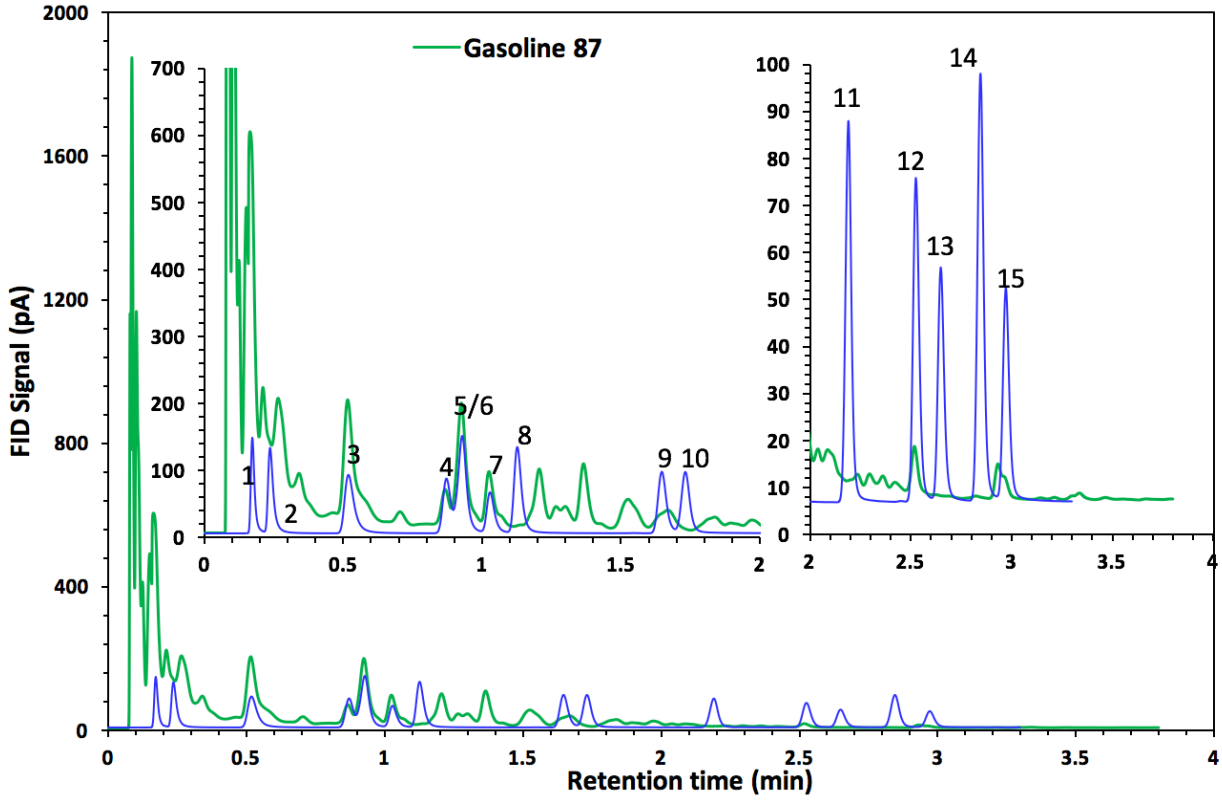

Figure S 4: Overlay of the chromatograms of the separation of gasoline (green) and 15-component standard mixture (blue). The separation conditions for both the runs are the same (as in Fig. S3 and Fig. 4a). Insets show the magnified view of the selected regions. Peak numbers in the standard mixture correspond to 1) heptane, 2) benzene, 3) toluene, 4) ethylbenzene, 5/6) p- and m-xylenes, 7) o-xylene, 8) styrene, 9) benzyl chloride, 10) 1,2-dichlorobenzene, 11) 1,2,4-trichlorobenzene, 12) naphthalene, 13) 2-nitrotoluene, 14) 3-nitrotoluene, and 14) 4-nitrotoluene.

Compound	For [P66614][NTf2]-coated column	For [BPyr][NTf2]-coated column
Heptane	1.64	1.73
Benzene	1.73	1.47
Toluene	1.62	1.44
Ethylbenzene	na	1.32
p/m-Xylenes	1.22	1.14
o-Xylene	1.34	1.36
Styrene	1.37	1.21
Benzyl chloride	1.29	1.33
1,2-Dichlorobenzene	1.09	1.21
1,2,4-Trichlorobenzene	1.12	1.09
Naphthalene	1.22	1.26
2-Nitrotoluene	1.22	1.20
3-Nitrotoluene	1.13	1.09
4-Nitrotoluene	1.19	1.17

Table S 1: Peak tailing factors for different compounds

Compound	For [P66614][NTf2]-coated column	For [BPyr][NTf2]-coated column
C8:00	1.72	1.36
C10:00	1.46	1.34
C12:00	1.45	0.92
C14:00	1.76	1.27
C16:00	1.71	1.53
C18:00	na	1.40
C18:01	na	1.39
C18:02	na	1.44

Table S 2: Peak tailing factors for Fatty Acid Methyl Esters

3.6.1. References

[1] J.M. Rankin, K.S. Suslick, The development of a disposable gas chromatography microcolumn, Chem. Commun., 51 (2015) 8920-8923.

[2] S. Ali, M. Ashraf-Khorassani, L.T. Taylor, M. Agah, MEMS-based semi-packed gas chromatography columns, Sens. Actuators, B, 141 (2009) 309-315.

[3] H. Shakeel, M. Agah, High density semipacked separation columns with optimized atomic layer deposited phases, Sens. Actuators, B, 242 (2017) 215-223.

[4] S. Reidy, G. Lambertus, J. Reece, R. Sacks, High-performance, static-coated silicon microfabricated columns for gas chromatography, Anal. Chem., 78 (2006) 2623-2630.

[5] M. Stadermann, A.D. McBrady, B. Dick, V.R. Reid, A. Noy, R.E. Synovec, O. Bakajin, Ultrafast gas chromatography on single-wall carbon nanotube stationary phases in microfabricated channels, Anal. Chem., 78 (2006) 5639-5644.

[6] H. Yuan, X. Du, H. Tai, Y. Li, X. Zhao, P. Guo, X. Yang, Y. Su, Z. Xiong, M. Xu, The effect of the channel curve on the performance of micromachined gas chromatography column, Sens. Actuators, B, 239 (2017) 304-310.

[7] A.D. Radadia, R.D. Morgan, R.I. Masel, M.A. Shannon, Partially buried microcolumns for micro gas analyzers, Anal. Chem., 81 (2009) 3471-3477.

[8] M. Agah, J.A. Potkay, G. Lambertus, R. Sacks, K.D. Wise, High-performance temperature-programmed microfabricated gas chromatography columns, J. Microelectromech. Syst., 14 (2005) 1039-1050.

[9] A. Garga, M. Akbar, E. Vejerano, S. Narayanan, L. Nazhandali, L.C. Marr, M. Agah, Zebra GC: A mini gas chromatography system for trace-level determination of hazardous air pollutants, Sens. Actuators, B, 212 (2015) 145-154.

[10] S. Zampolli, I. Elmi, F. Mancarella, P. Betti, E. Dalcanale, G. Cardinali, M. Severi, Real-time monitoring of sub-ppb concentrations of aromatic volatiles with a MEMS-enabled miniaturized gas-chromatograph, Sens. Actuators, B, 141 (2009) 322-328.

[11] Defiant Technologies, http://www.defiant-tech.com/frog-4000.php.

[12] APIX Analytics, http://www.apixanalytics.com/technology/.

[13] B. Alfeeli, S. Narayanan, D. Moodie, P. Zellner, M. McMillan, D. Hirtenstein, G. Rice, M. Agah, Interchannel Mixing Minimization in Semi-Packed Micro Gas Chromatography Columns, IEEE Sens. J., 13 (2013) 4312-4319.

[14] J. Vial, D. Thiébaut, F. Marty, P. Guibal, R. Haudebourg, K. Nachef, K. Danaie, B. Bourlon, Silica sputtering as a novel collective stationary phase deposition for microelectromechanical system gas chromatography column: Feasibility and first separations, J. Chromatogr. A, 1218 (2011) 3262-3266.

[15] J. Sun, D. Cui, F. Guan, X. Chen, L. Zhang, High resolution microfabricated gas chromatography column with porous silicon acting as support, Sens. Actuators, B, 201 (2014) 19-24.

[16] Y. Li, R. Zhang, T. Wang, Y. Wang, Y. Wang, L. Li, W. Zhao, X. Wang, J. Luo, A micro gas chromatography with separation capability enhanced by polydimethylsiloxane stationary phase functionalized by carbon nanotubes and graphene, Talanta, 154 (2016) 99-108.

[17] Y. Li, X. Du, Y. Wang, H. Tai, D. Qiu, Q. Lin, Y. Jiang, Improvement of column efficiency in MEMS-Based gas chromatography column, RSC Adv., 4 (2014) 3742-3747.

[18] T. Nakai, S. Nishiyama, M. Shuzo, J. Delaunay, I. Yamada, Micro-fabricated semi-packed column for gas chromatography by using functionalized parylene as a stationary phase, J. Micromech. Microeng., 19 (2009) 065032.
[19] M.A. Zareian-Jahromi, M. Agah, Microfabricated gas chromatography columns with monolayer-protected gold stationary phases, J Microelectromech. Syst., 19 (2010) 294-304.
[20] H. Shakeel, M. Agah, Semipacked separation columns with monolayer protected gold stationary phases for microgas chromatography, Sensors, IEEE, 2012, pp. 1-4.
[21] H. Shakeel, D. Wang, J.R. Heflin, M. Agah, Improved self-assembled thiol stationary phases in microfluidic gas separation columns, Sens. Actuators, B, 216 (2015) 349-357.
[22] V.R. Reid, M. Stadermann, O. Bakajin, R.E. Synovec, High-speed, temperature programmable gas chromatography utilizing a microfabricated chip with an improved carbon nanotube stationary phase, Talanta, 77 (2009) 1420-1425.
[23] G. Lambertus, A. Elstro, K. Sensenig, J. Potkay, M. Agah, S. Scheuering, K. Wise, F. Dorman, R. Sacks, Design, fabrication, and microfabricated columns evaluation of for gas chromatography, Anal. Chem., 76 (2004) 2629-2637.
[24] A.D. Radadia, R.I. Masel, M.A. Shannon, J.P. Jerrell, K.R. Cadwallader, Micromachined GC columns for fast separation of organophosphonate and organosulfur compounds, Anal. Chem., 80 (2008) 4087-4094.
[25] D. Read, C.H. Sillerud, Metal-Organic Framework Thin Films as Stationary Phases in Microfabricated Gas-Chromatography Columns, in, Sandia National Laboratories (SNL-NM), Albuquerque, NM (United States), 2016.
[26] H. Shakeel, G.W. Rice, M. Agah, Semipacked columns with atomic layer-deposited alumina as a stationary phase, Sens. Actuators, B, 203 (2014) 641-646.
[27] M. Akbar, H. Shakeel, M. Agah, GC-on-chip: integrated column and photoionization detector, Lab Chip, 15 (2015) 1748-1758.
[28] R. Haudebourg, Z. Matouk, E. Zoghlami, I. Azzouz, K. Danaie, P. Sassiat, D. Thiebaut, J. Vial, Sputtered alumina as a novel stationary phase for micro machined gas chromatography columns, Anal. Bioanal. Chem., 406 (2014) 1245-1247.
[29] R. Haudebourg, J. Vial, D. Thiebaut, K. Danaie, J. Breviere, P. Sassiat, I. Azzouz, B. Bourlon, Temperature-programmed sputtered micromachined gas chromatography columns: An approach to fast separations in oilfield applications, Anal. Chem., 85 (2012) 114-120.
[30] D. Wang, H. Shakeel, J. Lovette, G.W. Rice, J.R. Heflin, M. Agah, Highly Stable Surface Functionalization of Microgas Chromatography Columns Using Layer-by-Layer Self-Assembly of Silica Nanoparticles, Anal. Chem., 85 (2013) 8135-8141.
[31] R. Hayes, G.G. Warr, R. Atkin, Structure and nanostructure in ionic liquids, Chem. Rev., 115 (2015) 6357-6426.
[32] J.L. Anderson, D.W. Armstrong, High-stability ionic liquids. A new class of stationary phases for gas chromatography, Anal. Chem., 75 (2003) 4851-4858.
[33] J.L. Anderson, D.W. Armstrong, Immobilized ionic liquids as high-selectivity/high-temperature/high-stability gas chromatography stationary phases, Anal. Chem., 77 (2005) 6453-6462.
[34] S.K. Poole, P.H. Shetty, C.F. Poole, Chromatographic and spectroscopic studies of the solvent properties of a new series of room-temperature liquid tetraalkylammonium sulfonates, Anal. Chim. Acta, 218 (1989) 241-264.

[35] R.M. Pomaville, C.F. Poole, Solute-solvent interactions in liquid tetrabutylammonium sulfonate salts studied by gas chromatography, Anal. Chem., 60 (1988) 1103-1108.
[36] J.L. Anderson, R. Ding, A. Ellern, D.W. Armstrong, Structure and properties of high stability geminal dicationic ionic liquids, J. Am. Chem. Soc., 127 (2005) 593-604.
[37] C.D. Tran, S. Challa, Fullerene-impregnated ionic liquid stationary phases for gas chromatography, Analyst, 133 (2008) 455-464.
[38] Z.S. Breitbach, D.W. Armstrong, Characterization of phosphonium ionic liquids through a linear solvation energy relationship and their use as GLC stationary phases, Anal. Bioanal. Chem., 390 (2008) 1605-1617.
[39] C. Guerrero-Sanchez, T. Erdmenger, T. Lara-Ceniceros, E. Jimenez-Regalado, U.S. Schubert, Smart materials based on ionic liquids: the magnetorheological fluid case, in: ACS symposium series, Oxford University Press, 2009, pp. 147-155.
[40] M. Deetlefs, K.R. Seddon, Ionic liquids: fact and fiction, Chim. Oggi, 24 (2006).
[41] J.L. Anderson, J. Ding, T. Welton, D.W. Armstrong, Characterizing ionic liquids on the basis of multiple solvation interactions, J. Am. Chem. Soc., 124 (2002) 14247-14254.
[42] C.F. Poole, S.K. Poole, Ionic liquid stationary phases for gas chromatography, J. Sep. Sci., 34 (2011) 888-900.
[43] L.W. Hantao, A. Najafi, C. Zhang, F. Augusto, J.L. Anderson, Tuning the selectivity of ionic liquid stationary phases for enhanced separation of nonpolar analytes in kerosene using multidimensional gas chromatography, Anal. Chem., 86 (2014) 3717-3721.
[44] G.R. Lambertus, J.A. Crank, M.E. McGuigan, S. Kendler, D.W. Armstrong, R.D. Sacks, Rapid determination of complex mixtures by dual-column gas chromatography with a novel stationary phase combination and spectrometric detection, J. Chromatogr. A, 1135 (2006) 230-240.
[45] C. Ragonese, P.Q. Tranchida, D. Sciarrone, L. Mondello, Conventional and fast gas chromatography analysis of biodiesel blends using an ionic liquid stationary phase, J. Chromatogr. A, 1216 (2009) 8992-8997.
[46] W.R. Collin, A. Bondy, D. Paul, K. Kurabayashi, E.T. Zellers, μGC× μGC: comprehensive two-dimensional gas chromatographic separations with microfabricated components, Anal. Chem., 87 (2015) 1630-1637.
[47] B.P. Regmi, J. Monk, B. El-Zahab, S. Das, F.R. Hung, D.J. Hayes, I.M. Warner, A novel composite film for detection and molecular weight determination of organic vapors, J. Mater. Chem., 22 (2012) 13732-13741.
[48] C. Kulsing, Y. Nolvachai, H.M. Huegel, P.J. Marriott, Developments in gas Chromatography using ionic liquid stationary phases, LCGC Eur., 28 (2015) 434-440.
[49] J. W. Dolan. Why do peaks tail. LCGC Eur., 21, (2003): 612-616.

4. Semi-packed Gas Chromatography Column with Density Modulated Pillars

(Part of this chapter reproduced with permission from IEEE TRANSDUCERS)
R. Chan, A. Lopez, B. P. Regmi, and M. Agah, "Micro-pillar density modulation in semi-packed MEMS column," in 2017 19th International Conference on Solid-State Sensors, Actuators and Microsystems (TRANSDUCERS), 2017, pp. 1528–1531.

4.1. Abstract

The separation column is the most important component which influences the performance of gas chromatography systems. Among a number of column designs, the microfabricated semi-packed column has attracted particular attention in micro gas chromatography because it enhances the separation efficiency and provides higher sample capacity compared to the open-channel counterparts. However, these added advantages comes at the cost of higher pressure drops per unit length of the separation column. This paper reports new semi-packed column designs through density modulation of the pillars by changing the spacing between rows or the number of pillars per row from. Various geometries were fabricated and tested against regular semi-packed columns having either one pillar or four pillars per row. Different performance metrics were measured including column pressure drop, optimal flow velocity, number of theoretical plates, and separation efficiency. The density-modulated semi-packed columns provide efficiencies

comparable to that of semi-packed columns embedding more pillars per row while requiring a lower inlet pressure which is more comparable to the columns embedding one pillar per row. These density-modulated columns were able to successfully separate diesel and kerosene compounds and to identify the major hydrocarbon constituents of these two widely used samples.

4.2. Introduction

Gas chromatography (GC) is used in a variety of fields where the monitoring of volatile organic compounds (VOCs) is of importance [1]. Standard GC tools and systems are bulky and consume high power during operation. The current trend in this field is moving towards miniaturizing the system to allow for field and point-of-care usage. Microsystems-based GCs allow for great portability, reduced sampling and analysis times, and lower power consumptions [2]–[8].

The heart of a GC is the column which is responsible for the separation of different components of a mixture before detection. The separation is due to differential interaction of the components of a mixture with the stationary phase coating of the column. As the compounds of the mixture flow through the separation column, they spend the same time in the inert carrier gas that pushes the sample through the column. However, they adsorb or desorb at different rates depending on their affinity to the stationary phase. This affects the time that spend by each compound in the stationary phase and hence affecting the overall time required for each compound to pass through the entire column. The compounds separated in time and space are then detected at the outlet of the column as they pass over a detector and their chromatographic response can be recorded. In most GCs, the separation column is an open tubular fused silica capillary tubing having a stationary phase on its inner wall. Changing the length of the column or the stationary phase coating will

subsequently change the behavior of the column and the GC separation performance including the resolution, peak shape and capacity, and separation selectivity.

The development of planar columns fabricated using microelectromechanical systems (MEMS) technology is a solution for reducing the footprint of the separation component, for reducing cost through batch fabrication, for integrating heaters and temperature sensors for fast and complex analysis, and for decreasing overall size and power requirements. Different research groups are working to develop different geometries, topographies, and stationary phases in order to improve the chromatographic performance of MEMS columns [9]–[13]. Early work in this area were primarily focused on simple microfluidic channels etched in silicon and bonded to a Pyrex wafer [7], [14], [15]. These column cross sections were determined based on the type of etch performed to create the channels defined by photolithography techniques. Depending on the etching method used, these channels had either rectangular or more circular cross sections [7], [16]. These early columns were typically coated with conventional stationary phases such as OV-1 to mimic a planar and miniaturized version of the open tubular columns used in conventional GCs [7], [14], [17].

In an attempt to improve the performance of these early micro columns (μCs), research was directed at changing the geometries and topographies of the micro-channels to improve upon different parameters. The multi-capillary μC design first introduced by our group was developed in order to improve upon the separation efficiency without sacrificing sample capacity [18]. This was based off of the Golay equation which indicates that reduction in sample capacity by decreasing the inner-diameter of a column can be compensated by increasing the number of parallel capillaries [19]. The work showed that a column consisting of four parallel channels 65μm

wide provided a sample capacity twenty times that of a single 50μm wide channel. However, it also noted that conventional coating techniques failed to produce a high yield when multi-capillary columns with a large number of parallel capillaries were used.

Among different MEMS-enabled columns, the semi-packed columns (SPCs), also reported by our group, provide improved separation efficiency and sample capacity when compared to their open rectangular counterparts [20]. In addition, it also helps to suppress the coating issues faced in multi-capillary configurations. By embedding pillars into the channel, the effective channel width is reduced and the internal surface area is increased. This allows for easier coating using established conventional coating techniques as there is a larger single volume compared to multiple smaller volumes. The increase in surface area also allows for more of the stationary phase coating thereby increasing the sample capacity. The embedded pillars also reduce the distance of mass transfer which helps create a more uniform interaction between the mobile and stationary phases. Similarly, the flow velocity profile is also more uniform after including the embedded pillars which can reduce band broadening [20], [21]. Work is constantly being conducted with the hope of optimizing this semi-packed design. For example, several groups have reported on the effect of the pillar shape to generate a more even flow velocity profile [21]. Pillar density is also something that has been used to tune the separation efficiency [22]–[24]. Research has even been conducted on the shape of the channels and how it can affect the GC performance [10], [11], [25]. However, while the SPC design has a lower pressure requirement than the multi-capillary columns, they still have a much higher requirement compared to an open rectangular μC. This problem is exacerbated further when pillar density is increased monotonically through the entire channel to further improve the separation efficiency [18], [22], [23].

Another μC design that has been reported by our group is the width-modulated column [9]. Compared to a standard open rectangular column, these width-modulated devices performed more favorably due to the change in the channel width over the length of the column. This is due to the separation efficiency being proportional to the square of the channel width. As the channel becomes smaller, the local separation efficiency increases which leads to the overall column becoming more efficient as a result [9]. Modulation of the column width or the thickness of stationary phase in a column is an old concept of GC dating back to 1962 where it is believed that diminishing the interaction between mobile and stationary phase could provide similar effects as temperature or pressure programming [26]. Following our previous work, this paper reports a new μC design based on the combination of two MEMS column topographies: SPC and width modulation. These designs demonstrate that instead of using a high density of pillars in an SPC, a modulation of the pillar density over the length of the column can result in high resolution separations of complex mixtures without requiring high pressures when compared to semi-packed columns having a high density of pillars. Even though the focus of this paper is the development of new MEMS GC columns, it is worth mentioning that the columns reported here are coated with a room-temperature ionic liquid. These stationary phases offer unique separation capabilities and their successful integration with MEMS columns have already been demonstrated [27].

4.3. Column Design and Fabrication

4.3.1. Design

Four distinct density modulated semi-packed columns (DMSPC) as indicated in Table 1 along with two regular semi-packed columns as control geometries were designed and fabricated in this work. These new DMSPCs relies upon the embedded micro-pillars to improve the separation efficiency over a standard open rectangular column but does so in a way that does not require the same pressure requirements of semi-packed columns with high density pillars. This density modulation was achieved by creating different modulation approaches for the embedded pillars. The length and width of the columns for all these cases were kept at 1 m and 190 μm, respectively. Design A and B in Table 1 are based on changing the row pitch between the embedded pillars. Figure 1a shows a top-down scanning electron microscopy (SEM) view of these scenarios. Specifically, the row pitch changes from 120μm at its least dense, to 80μm row pitch spacing, to 40μm at its most dense. Added to that, the number of pillars also alternates between three and four as seen in Figure 1a. The combination of row pitch and the number of pillars create six different topographies. In Design A, the entire column length is divided into 6 sections and each section has one of the above topographies. In Design B, every 10 cm of the column length has all those 6 topographies and then repeats itself. The details of these designs can be found in supplementary documents. In both Design A and B, where the local volume is larger, there is less flow resistance due to reduced number of the embedded pillars. As the density of the embedded pillars increases, however, the local separation efficiency improves. Designs C and D take advantage of the concept of "virtual walls" in semi-packed columns [28]. These virtual walls are dependent on the row pitch spacing. In these designs, a row pitch of 40μm was maintained through the column length but

modulation achieved by varying the number of pillars per row from one to five as seen in Figure 1b. Design C mirrors the width modulation in that the density of the embedded pillars is lowest at the inlet and transitions to the highest density over the length of the column. Each 20 cm of the column length has the same number of pillars per row. Design D follows the repeated topography. More specifically, the first 10cm of the column length is divided into 5 equal sections where each section has a specific number of pillars per row. This pattern repeats itself through the length of the column. The details of Design C and D can also be found in the supplementary documents.

DMSPC Variation	Topography	Geometry
A	Row pitch spacing	Low to high
B	Row pitch spacing	Repeated
C	Pillars per row	Low to High
D	Pillars per row	Repeated

Table 4.1: Different density modulated semi-packed column design variations of topography and geometry.

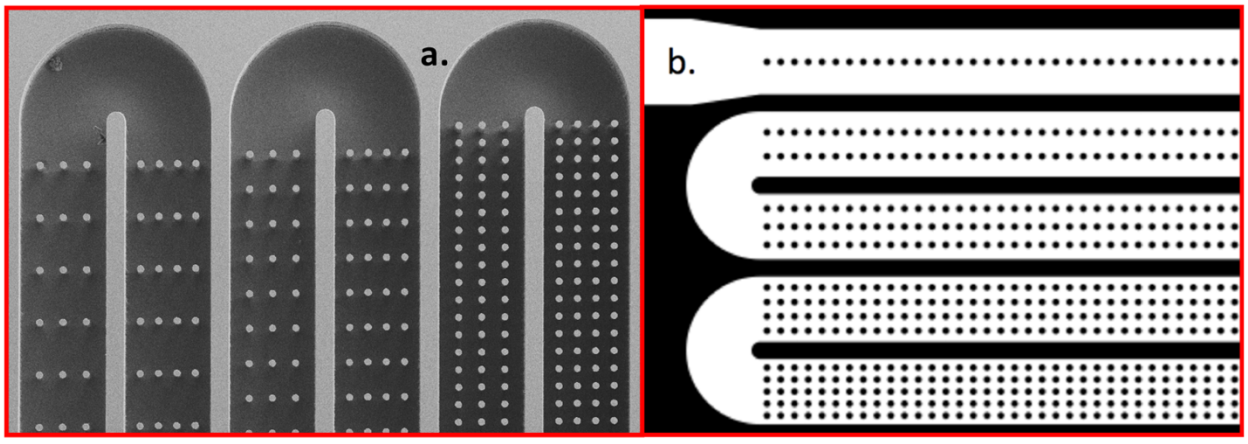

Figure 4.1: (a) SEM of DMSPC using pillar row distance to modulate density, (b) portion of mask showing DMSPC using number of pillars to modulate density.

4.3.2. Fabrication

The fabrication process for these devices is similar to previously reported columns [3], [29]. Silicon wafers (100 orientation, n-type, 4 inch diameter, 500µm thickness, single side polished, purchased from UniversityWafer, 11 Elkins Street, Unit 330, South Boston, MA 02127) were prepared for photolithography with a solvent clean and adhesion promoter hexamethyldisilazane (HMDS). AZ 9260 photoresist (purchased from Integrated Micro Materials, 8141 Gateway Drive, Suite 240, Argyle, Texas 76226) was spun on the wafers and patterned to expose the channels for the devices. The etching was accomplished by utilizing deep reactive ion etching (DRIE) and the Bosch process. By alternating between sulfur hexafluoride ([SF_6]) as the etch gas and octafluorocyclobutane ([C_4F_8]) as the passivation gas, an anisotropic etch is achieved to a depth of 240µm. Excess photoresist is stripped using a combination of acetone, isopropyl alcohol, and oxygen plasma. A 10nm film of aluminum oxide ([Al_2O_3]) is then deposited using atomic layer deposition (ALD). Trimethylaluminum ([$Al_2(CH_3)_6$]) and water were used as precursors for this process. Afterwards, a Pyrex wafer (purchased from UniversityWafer) is anodically bonded to the silicon wafer to create an airtight seal, completing the micro-channels used as the separation column. After dicing the wafer stack, fused silica micro-capillaries (purchased from Polymicro Technologies, 18019 N25th Ave, Phoenix, AZ 85023) were connected using Miller-Stephenson Epoxy 907 (purchased from Miller-Stephenson, 6321 W. Dempster St. #302, Morton Grove, IL 60053) to complete the devices. After curing the epoxy and testing for leaks, the devices were coated with 2mg/ml of a room temperature ionic liquid: 1-butyl-3-methylimidazolium hexafluorophosphate ([BMIm][PF_6]) in acetone. The use of ionic liquids allows for very fine-tuning when it comes for applying them for a specific application. This allows for very fine-tuning when it comes for applying them for a specific application. Recently, we have shown that these

materials can perform as suitable stationary phases in MEMS separation columns to separate non-polar and polar compounds with robust temperature stability [27]. The columns were coated using conventional static coating techniques. The final dimensions for the device are: 1m long, 190μm wide, 240μm deep, with 20μm embedded micro-pillars. Figures 2a and 2b show optical images of these completed devices. It should be noted that the color of the channels indicates the density of the pillars in those regions as the less dense channels reflect more light than the more dense channels. Figures 2c and 2d are SEM images of the cross sections of a portion of each devices.

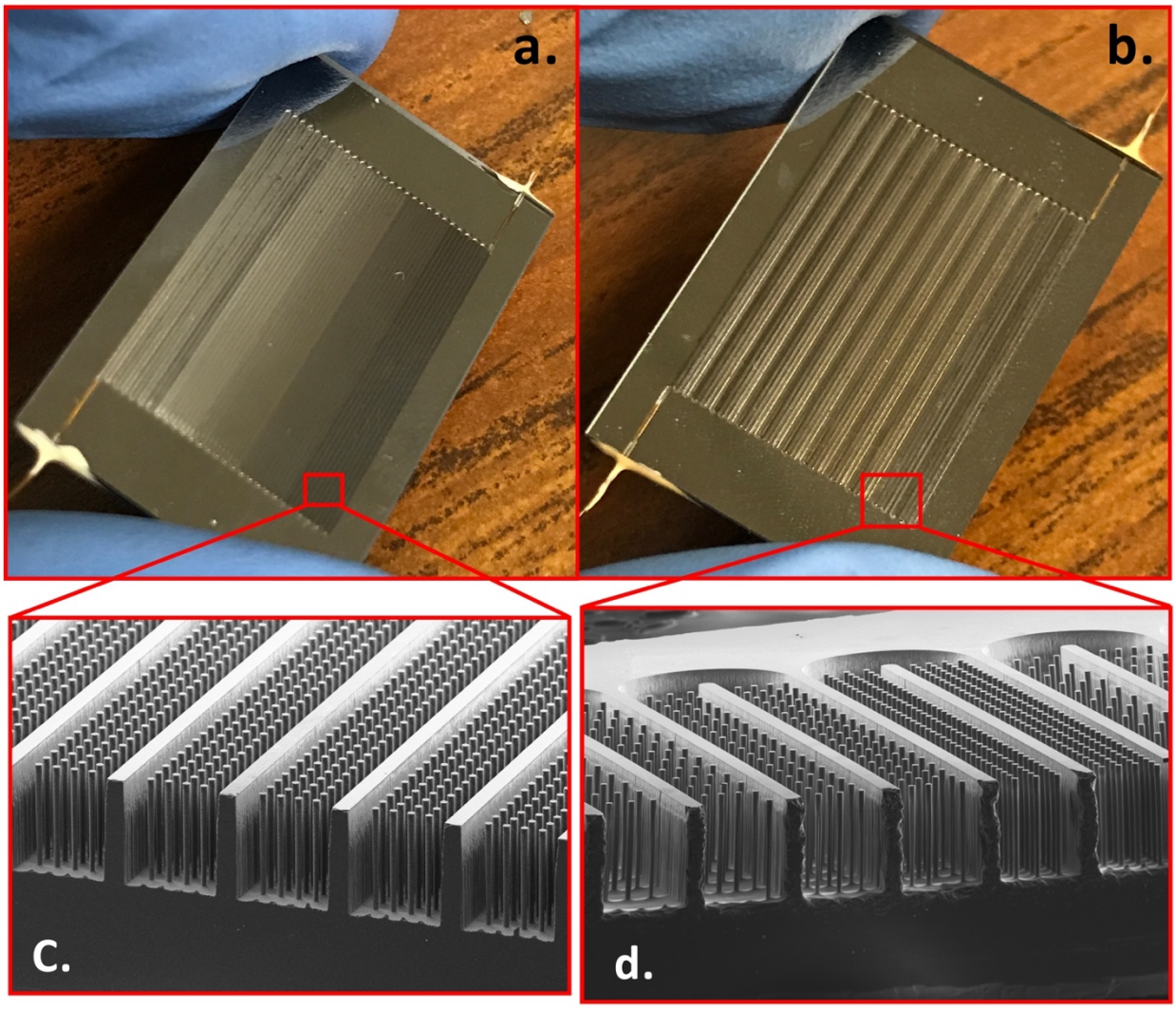

Figure 4.2: (a) optical image of low density to high density geometry, (b) optical image of repeated density geometry, (c) isometric SEM image showing no change in pillar density, (d) isometric SEM image showing change in pillar density. Notice the color of the channels in the optical images as they indicate the density of that portion. Darker is more dense, lighter is less dense.

4.4. Experimental and Analytical Methods

4.4.1. Experimental Setup

Total volumetric flow through these devices was measured using an Agilent ADM 1000 Flowmeter at varying inlet pressures. The separation performance of these MEMS columns were evaluated using the Agilent 7890A GC-FID system. This GC system is equipped with two flame ionization detectors (FID), an automated liquid sampler (7693A) for precisely controlling injection sample size, and a conventional GC oven. For the duration of the tests, both the injector and detector were set to a temperature of 280 °C. Ultra high purity helium was used as the carrier gas for the experiments. The micro-capillary fluidic connections were fused silica capillary tubes with a total length of 30cm. Prior to testing, each device was conditioned in the GC system by flowing helium through it at an inlet pressure of 10 psi while the temperature of the oven was increased from 30°C to 130°C at a rate of 2°C/min.

4.4.2. Analysis Approach

Theoretical flow analysis of these columns were conducted through COMSOL Multiphysics software simulations. Figure 3 shows gas flow simulations through a channel with different micro-pillar pitch sizes. To generate these results, a pressure is applied to the bottom of the channel segments and the flow velocity is measured. As mentioned earlier, these simulation results indicate what is known as a "virtual wall." These virtual walls which can be seen in Figure 3b indicate that the pillars with a row pitch of 40µm exhibit close to zero flow between the pillars along the length of the channel. The sections with row pitches larger than 40µm show more flow between rows of

pillars indicating an increase in intra-channel mixing. This mixing is not beneficial as it can lead to more peak broadening which in turn reduces the separation column efficiency.

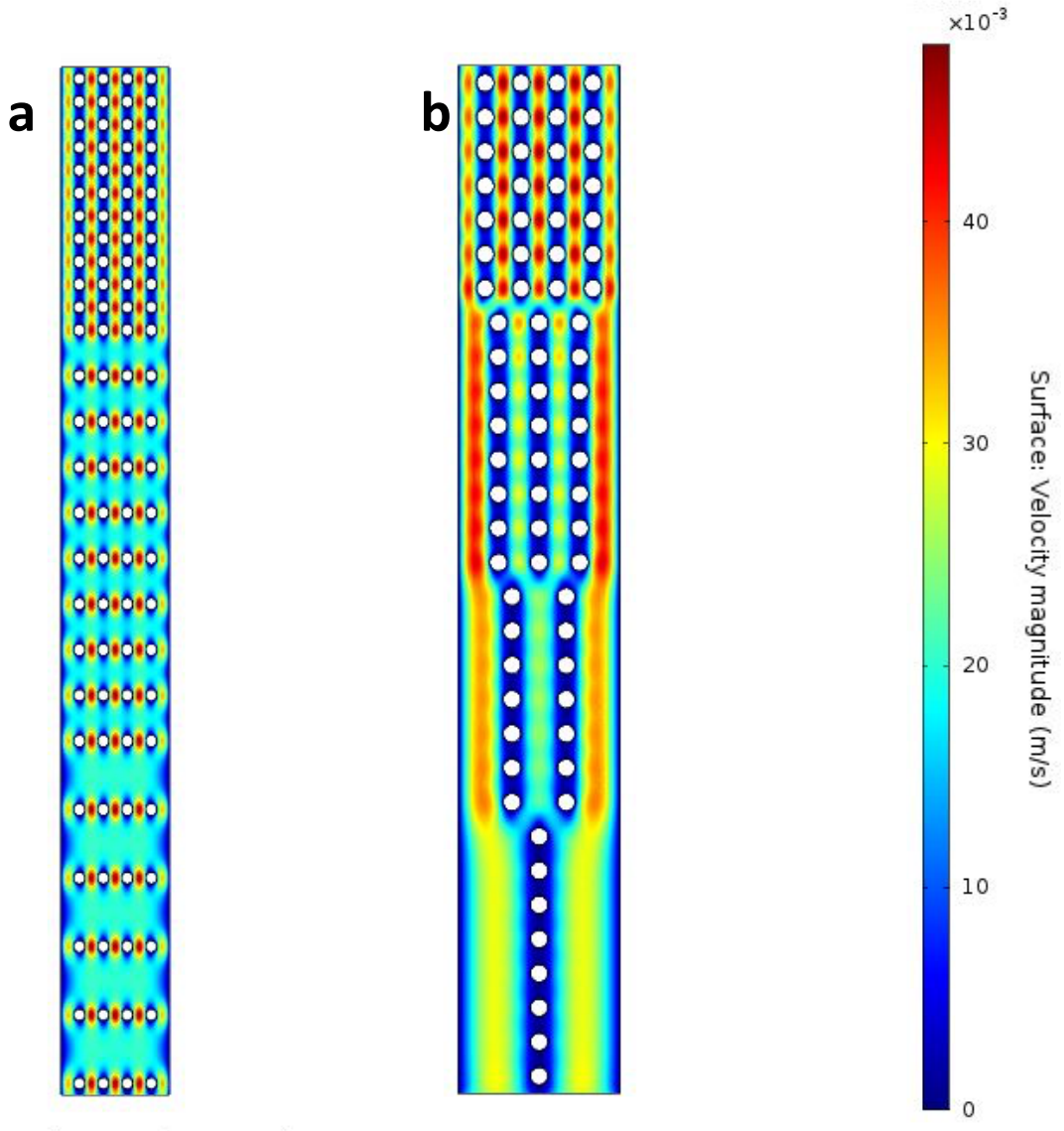

Figure 4.3: COMSOL Multiphysics software fluid flow simulations for micro-pillars in a channel with: (a) varying pitch distance, (b) varying number of pillars. Notice the dark blue areas indicating close to zero velocity between the pillars as the row pitch decreases.

For the same analyte, if a column produces more band broadening, it has less separation efficiency. This efficiency can be quantified by the number of theoretical plates (N) or the height-equivalent-to-a-theoretical-plate (H). The plate number at an isothermal temperature is a function of the stationary phase material and thickness, column dimensions, the velocity of carrier gas, the carrier gas properties, the inlet and outlet pressures, and the retention factor of the analyte of interest. Columns with larger plate numbers are considered to have better separation efficiency and better separation resolution [19]. H and N are related through the following equation:

$$H = \frac{L}{N} \qquad (1)$$

L is the column length. For a give column geometry and shape, the column efficiency is increased as the length of the column is increased. However, this comes at the cost of increased analysis time, increased pressure requirements, and increased power requirements when performing temperature programming to separate a wide range of anlaytes in term of boiling point. In our experiments, the objective is to compare different column geometries, and hence, we chose a MEMS column length of 1m for all different designs mentioned previously. In addition, we kept the column depth as 240μm and the total column width as 190μm. We should add there are established equations that relate H to column dimensions, stationary phase, carrier gas, and operating conditions. However, these theoretical models are derived for round capillary tubings for both open-tubular and packed columns used in conventional GCs and later were expanded to include open-rectangular MEMS columns. However, there is currently no theoretical equation derived by our group or others to predict the efficiency of semi-packed columns as there are multitude of parameters that can be varied in these columns. This issue will be even more

pronounced for our DMSPCs. Therefore, we used the experimental methods established in analytical chemistry to evaluate the separation efficiency of DMSPCs and control SPCs. The number of theoretical plates can be estimated by through the following equation:

$$N = 5.546 * \left(\frac{t_r}{w_h}\right)^2 \quad (2)$$

t_r is the retention time of the analye, and w_h is the width of the peak at half of its height. This equation indicates that a column is rewarded for retaining a peak for longer periods of time while still maintaining peak sharpness. For the purposes of this work, the plate number was calculated by using the Agilent ChemStation software bundled with the tool used. Normalization of the column efficiency with respect to its length is carried out through equation (1) and calculating *H* by using the measured *N* for each column. It is noteworthy that this method can be used if the analyte has a retention factor of 5 or more.

4.5. Results and Discussion

The performance of the DMSPCs were compared against the control designs that utilized the minimum density as well as the maximum density of pillars used in the DMSPCs. It should be noted that the effect of the different topographies and geometries on column performance is the focus of this paper not the stationary phase material or the coating technique. Figure 4 shows the results of testing the volumetric flow through each design as a function of different inlet pressures. What can be seen from the graph is that the design utilizing a minimum density of pillars throughout the column provides the most total volumetric flow at any given inlet pressure. This is

to be expected as it has more total volume due to a lower density of pillars than the rest of the designs. Similarly, the design with a maximum density of pillars has the lowest total flow rate at same pressure difference. Compared to these two extremes, all four DMSPC designs have very similar volumetric flow rates. Furthermore, the flow resistance of DMSPCs are closer to that of minimum control design. For instance, at 10psi, the volumetric flow rate through minimum control, DMSPCs, and maximum control are about 0.82 mL/min, 0.7 mL/min, and 0.33 mL/min, respectively. These numbers all indicate that for a given pressure the volumetric flow rate of DMSPCs is reduced only by 14% when compared to the minimum control design.

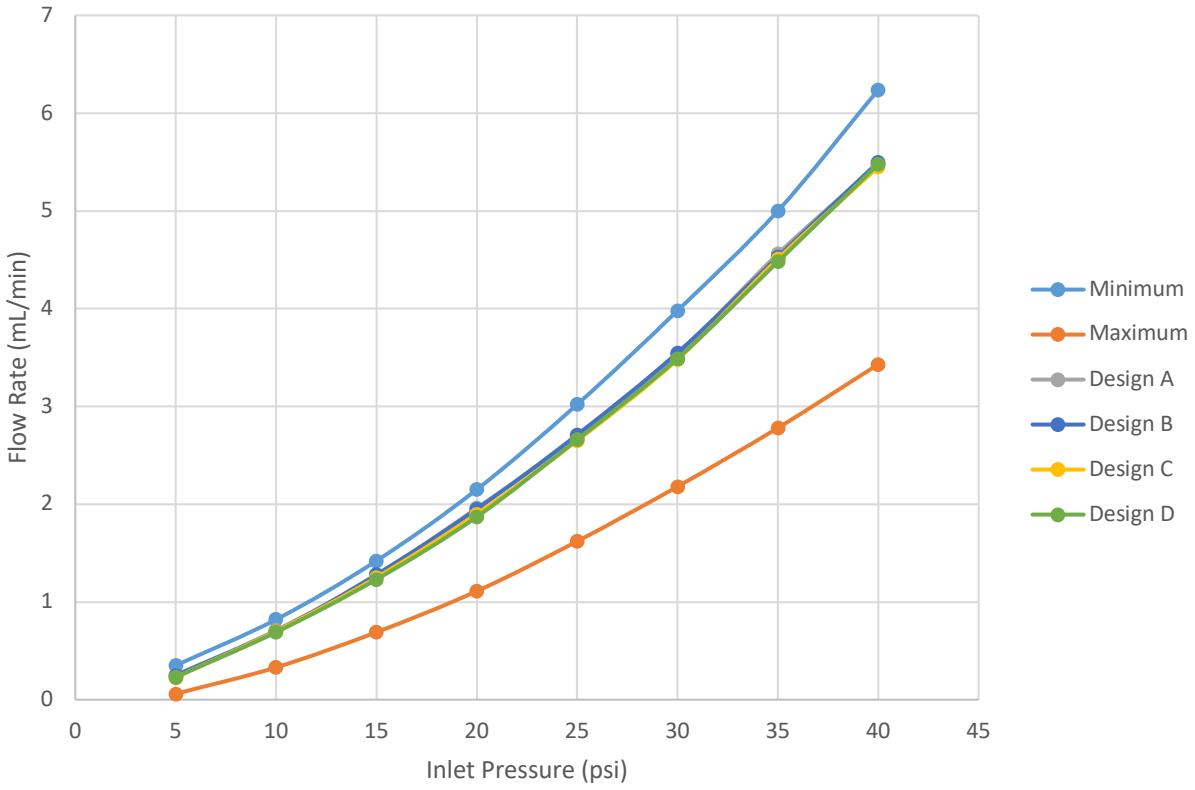

Figure 4.4: Graph showing the outlet flow rate versus the inlet pressure for the different column designs measured using an Agilent ADM 1000 Flowmeter. All four of the new density modulated designs are very similar and hard to distinguish.

Separation efficiency was calculated by using naphthalene as the test compound at 100˚C. Linear carrier gas velocity was measured by passing an un-retained methane peak and dividing the passage time by the length of the column and the micro-capillary connections. The Van Deemter plots generated from the results of these experiments can be seen in Figure 5. The average carrier gas flow velocity for the minimum control and maximum control at 10 psi pressure, for example, are 21.7 cm/s and 13.5 cm/s, respectively. For Design A, B, C, and D, the corresponding numbers are 14 cm/s, 15 cm/s, 14.2 cm/s, and 15.1 cm/s, respectively. The minimum density control shows the worst performance of the tested designs while the maximum density control shows the best overall performance when it comes to the plate numbers. These are expected as having a higher density of pillars creates a more uniform flow velocity between the rows of pillars and at the same time, minimizes the mass transfer distances [22], [24]. Figure 5a shows the separation efficiency comparison between Design A and Design B. Design A which utilizes the low-to-high density from inlet to outlet clearly produces a higher column efficiency when compared to Design B which has a density-modulation pattern that repeats itself over the length of the column. The same trend can be seen in Figure 5b when comparing the other two designs. Similar to Design B, Design D is based on the repeated arrangements of modulated pillar densities. This can be explained by looking at the generated peaks and their overall shape (not shown here). As an example, at a carrier gas flow velocity of 22cm/sec, the peak widths at half height for Designs A and B are 2.14 and 2.62 seconds, respectively, while both generating the same retention time of 22.7 seconds. The peak widths at half height for Designs C and D are 1.76 and 2.66 seconds, respectively, while both generating a retention time of 22.7 seconds, similar to Designs A and B. The peak width at half height for minimum and maximum control designs are 2.35 and 1.42 seconds, respectively. The

retention times are 21.5 and 26.6 seconds for minimum and maximum control designs. This indicates that the constant repetition from a low to high density of pillars, whether through modulation of the row pitch or the number of pillars per row, over the length of the column generates more band broadening when compared to designs that use low density at the inlet and transition to high density at the outlet. This is likely due to improved uniformity of the flow through the length of the column and reduced number of intermixing of the gas. Any transition between high density to low density results in sample mixing (see Figure 3) which in turn increases band broadening. Designs B and D include more number of such transitions. The effect of intermixing in monotonic semi-packed columns have been previously investigated by our group and discussed in [20]. In summary, Design A and Design C were identified as having a better performance than Design B and Design D. On the other hand, Design C yielded a higher separation efficiency when compared to Design A as revealed by Figure 5. At 22cm/s, Design A generates a peak width at half height which is 22% greater than that of Design C. It should be mentioned again that both designs produce the same retention time of 22.7 seconds. This increase in efficiency can be attributed to a smaller row pitch spacing and the presence of virtual walls in Design C. As can be seen in Figure 3, larger spacing between the rows in Design A increases the amount of interchannel mixing. Figure 6 shows two chromatograms generated by Design A and Design C, the two DMSPCs that exhibited the highest separation efficiency. The chromatographic conditions for these separations were: injection volume 0.1μL, split ratio of 400:1, inlet pressure of 10psi, oven temperature of 30˚C for 0.15min then ramped at a rate of 40˚C/min to 130˚C. The compounds separated were nine n-alkanes (purchased from Sigma-Aldrich, 3050 Spruce St., St. Louis, MO 63103) and are listed along with their boiling points in Table 2. The separation achieved by Design A shows a noticeable tailing for all the compounds while Design C creates more symmetrical

peaks. All of these results indicate that Design C as a separation column exhibits volumetric flow behavior more similar to that of the minimum density design while with regards to the separation efficiency, it behaves more like the maximum density design.

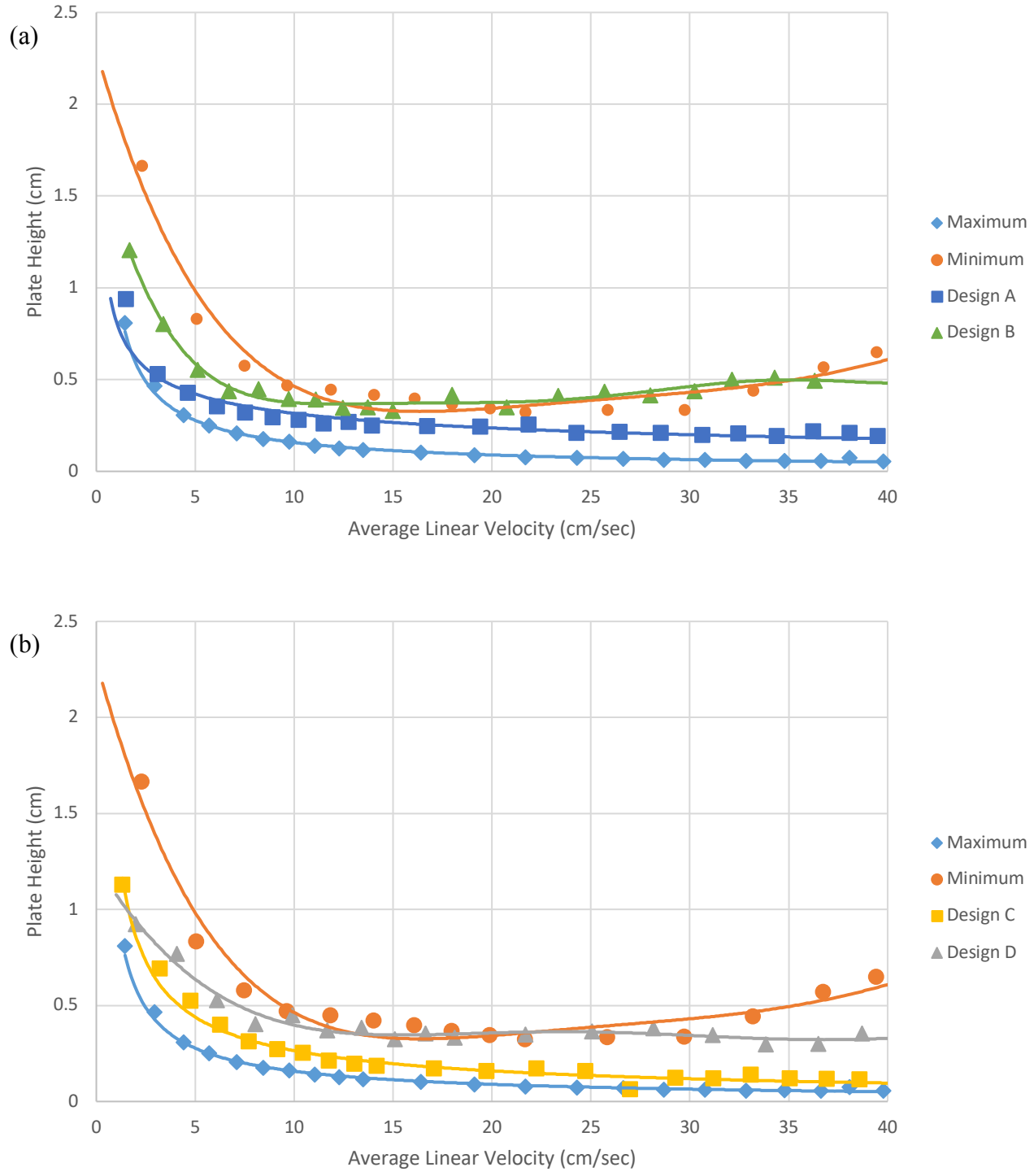

Figure 4.5: Van Deemter Plot showing the height-equivalent-to-a-theoretical-plate as a function of average linear velocity for (a) Design A and Design B, (b) Design C and Design D. Chromatographic conditions: injection volume 0.1µL, split ratio 100:1, oven temperature 100ºC, orientation of columns: low pillar density to high pillar density.

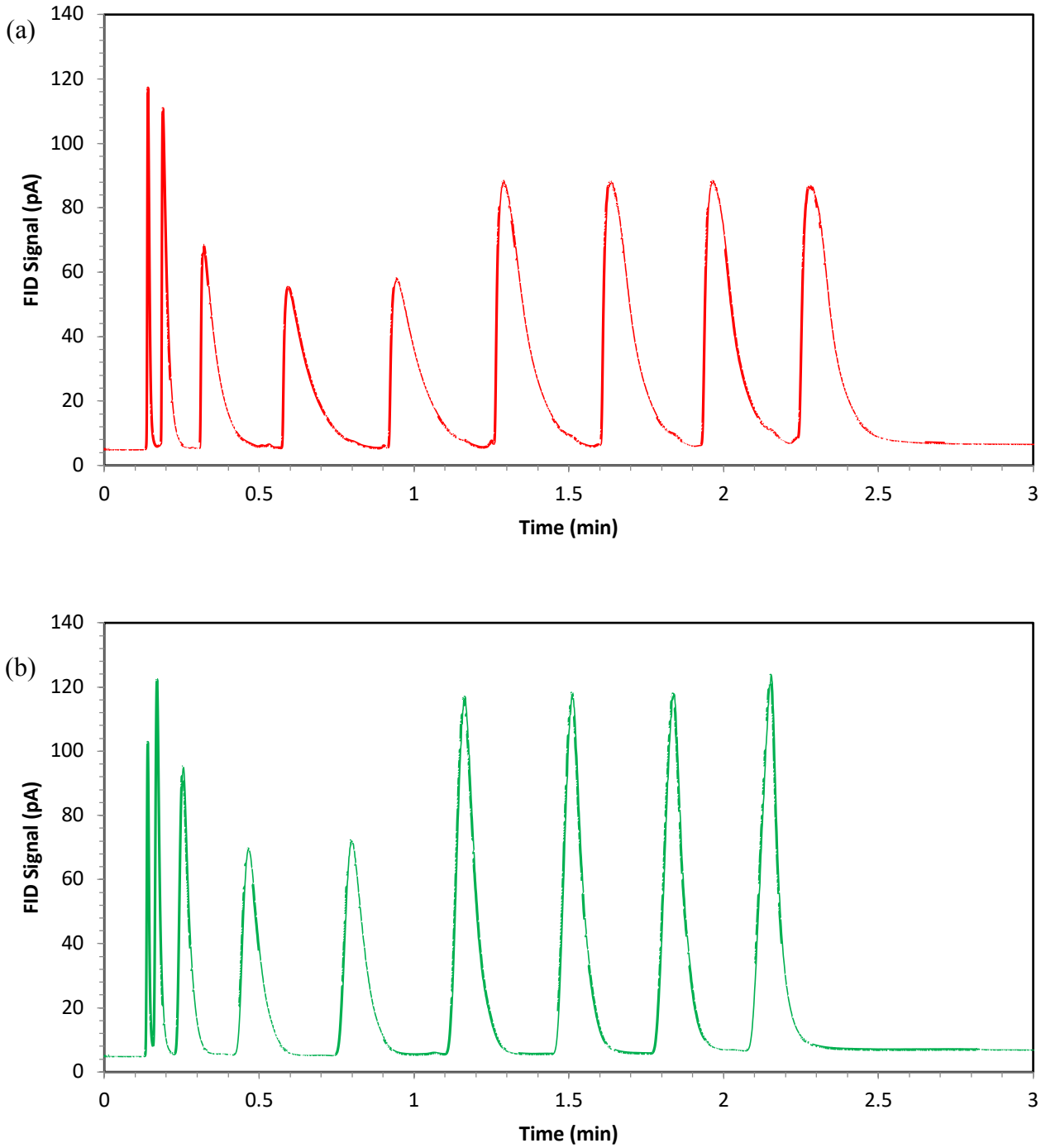

Figure 4.6: Separation of a mixture containing nine n-alkanes (heptane to pentadecane). Chromatographic conditions: injection volume 0.1µl, split ratio 400:1, inlet pressure 10psi, oven temperature 30˚C for 0.15 min and then ramped at the rate of 40˚C/min to 130˚C, orientation of the column: low pillar density to high pillar density. (a) 1st Gen ordered design, (b) 2nd Gen ordered design. Compound identification in order of elution: 1. Heptane, 2. Octane, 3. Nonane, 4. Decane, 5. Undecane, 6. Dodecane, 7. Tridecane, 8. Tetradecane, 9. Pentadecane.

Compounds	Boiling Point (ºC)
Heptane	98
Octane	126
Nonane	151
Decane	174
Undecane	196
Dodecane	216
Tridecane	235
Tetradecane	253
Pentadecane	270

Table 4.2: VOCs used in test mixtures for GC testing.

We used kerosene and diesel samples to demonstrate the efficiency of our DMSPC (Design C) for the separation of complex mixtures and compare its chromatographic performance with the control designs. Figure 7 shows a comparison of separations of kerosene at two different inlet pressures, 10psi and 40psi. The chromatographic conditions were: injection volume of 0.1μL, split ratio of 400:1, oven temperature of 30˚C for 0.15min then ramped at a rate of 40˚C/min to 130˚C. The chromatograms generated at 10psi show the differences in the overall time required to complete the separations. It can be seen that Design C generates a faster overall separation (Figure 7c) than the maximum density design (Figure 7a). However, it does not show a significant decrease in the resolution of the major hydrocarbon constituents when compared to the maximum density design. Interestingly, the behavior shown from the minimum density design shows a separation speed that is even slower than the maximum density design. This is thought to be due to the amount of stationary phase coating deposited in the channel compared to the other two designs because static coating techniques were used. The separations conducted at an inlet pressure of 40psi further highlight the lack of resolution change between the maximum density design (Figure 7b) and

Design C (Figure 7d). They also show the reduction of peak resolution in the minimum density design (Figure 7f) at higher inlet pressures. This is better visible in the inset of the 40psi separations. It is notable that the Van Deemter curves shown in Figure 5 associated with both Design C and maximum control design show a small variation of separation efficiency with respect to the column carrier gas flow velocity (pressure) above the optimal conditions (minimum H). However, the minimum control design shows a separation efficiency more comparable to open tubular and rectangular columns as the efficiency starts to decline as the velocity is raised above the optimal flow velocity. This can explain why the separation performance of the minimum control design is more dependent on the column pressure or flow velocity. Similar chromatograms generated from separating diesel at 10psi and 40psi are shown in Figure 8. The chromatographic conditions were the same as the kerosene separations but the analysis time were limited to five minutes to show the advantages of the DMSPC. Again, it can be seen that the separation from Design C occurs faster than the maximum density design. In this case, however, an extra analyte elutes from Design C when compared to the separation from the maximum density design. Similarly to the previous separations, the chromatograms from Design C do not show any significant reduction in peak resolution of major hydrocarbons in diesel mixture compared to the maximum density design. The results shown in these two figures indicate that DMSPC can generate a faster overall separation with the same inlet pressure when compared to the maximum density SPC. However, they do not show reduced resolution or separation efficiency, behavior that is more noticeable when compared against the minimum density design. These results can also indicate that DMSPC would require a lower inlet pressure to complete the same separation in the same fixed time period when compared to the maximum density SPC. This behavior will be beneficial as it relaxes the pumping requirements needed for micro GC systems.

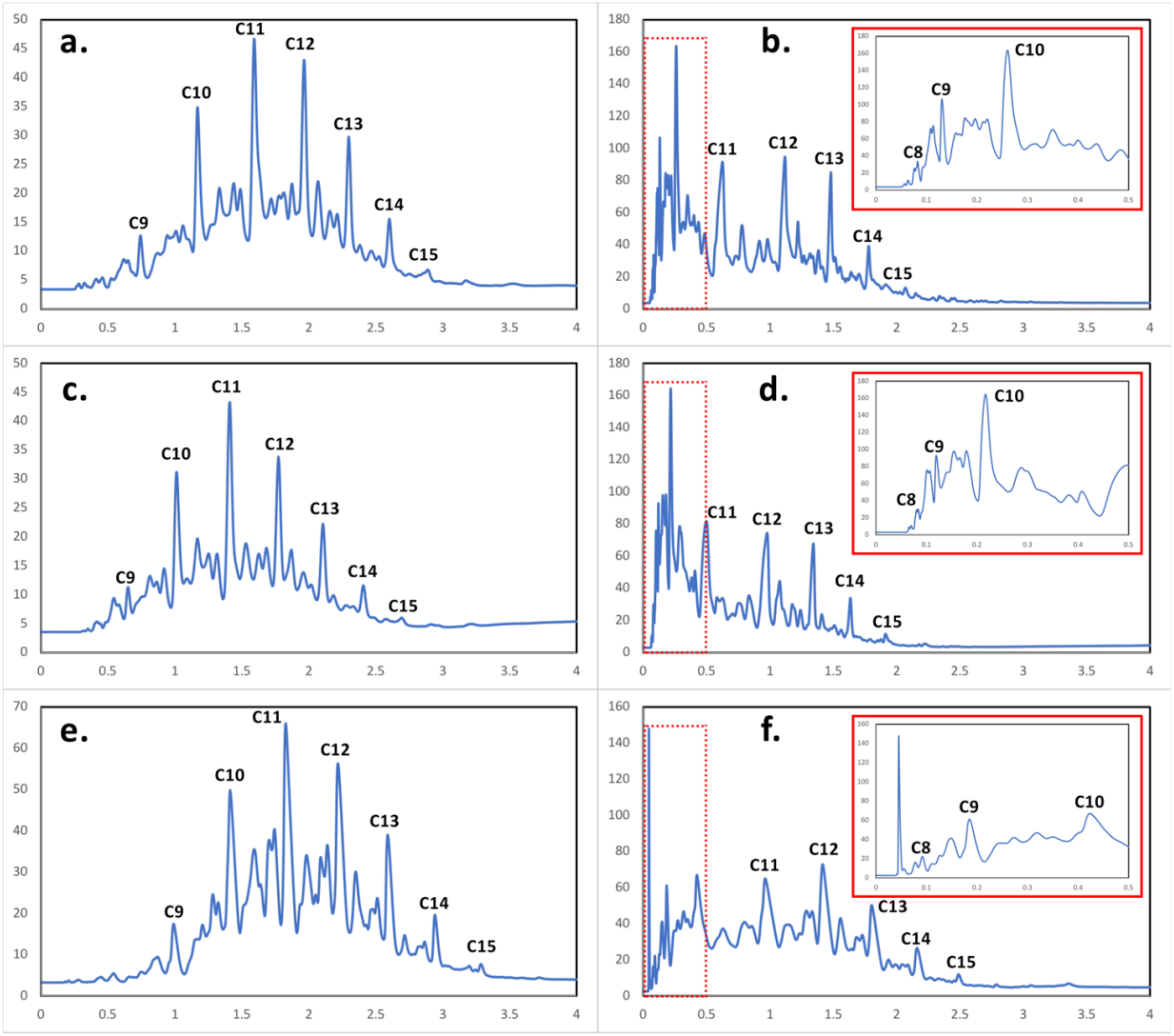

Figure 4.7: Kerosene separations conducted using the maximum density design (a, b), DMSPC Design C (c, d), and minimum density design (e, f). Separations were conducted at 10psi (a, c, e) and 40psi (b, d, f). Inset from 40psi separations shows resolution differences within first half minute of chromatogram. Chromatographic conditions: injection volume 0.1µl, split ratio 400:1, oven temperature 30˚C for 0.15 min and then ramped at the rate of 40˚C/min to 130˚C, orientation of the DMSPC column: low pillar density to high pillar density.

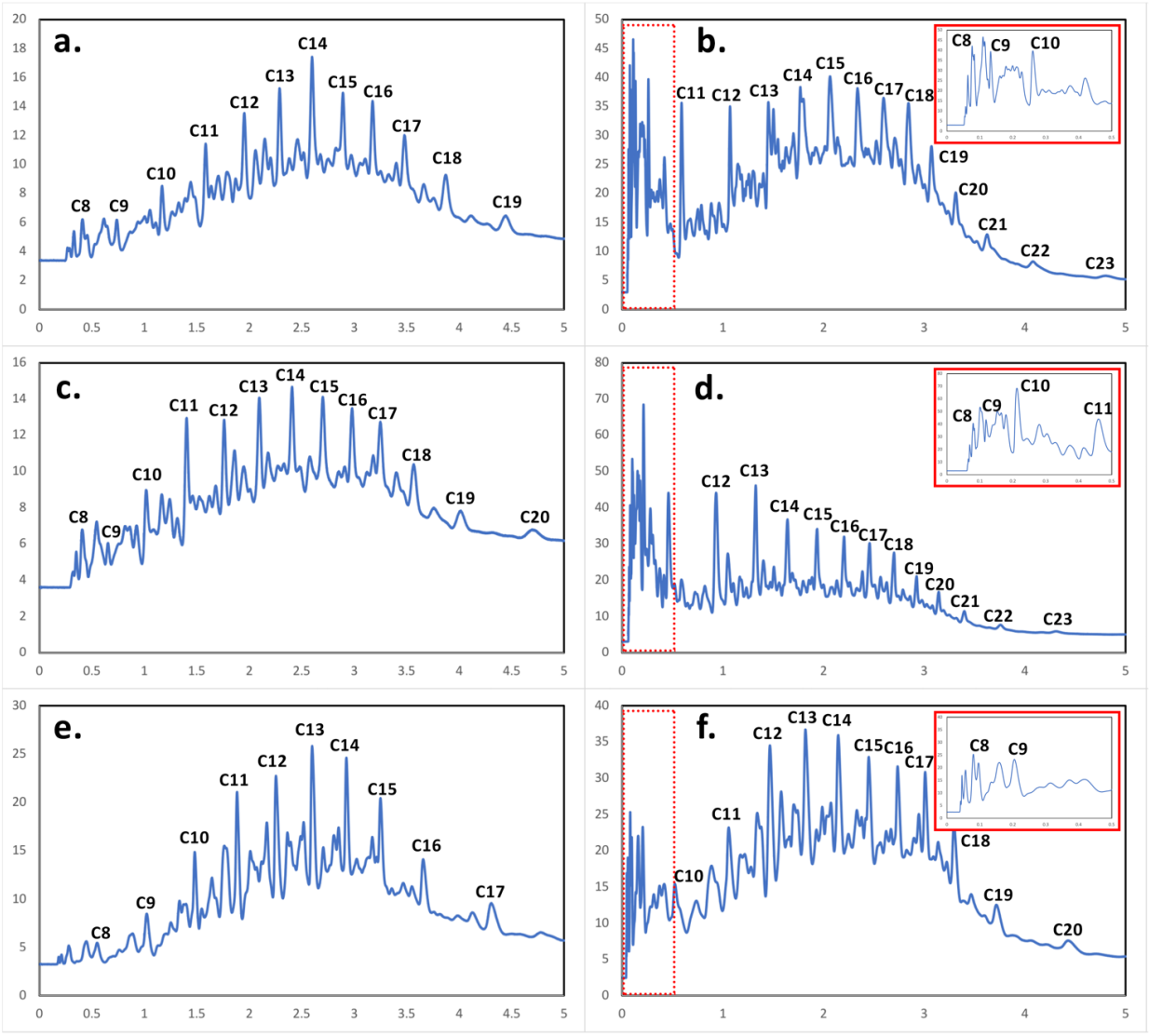

Figure 4.8: Diesel separations conducted using the maximum density design (a, b), DMSPC Design C (c, d), and minimum density design (e, f). Separations were conducted at 10psi (a, c, e) and 40psi (b, d, f). Inset from 40psi separations shows resolution differences within first half minute of chromatogram. Chromatographic conditions: injection volume 0.1µl, split ratio 400:1, oven temperature 30˚C for 0.15 min and then ramped at the rate of 40˚C/min to 130˚C, orientation of the DMSPC column: low pillar density to high pillar density.

4.6. Conclusion

In this work, we successfully developed new semi-packed MEMS separation columns utilizing pillar density modulation to increase total volumetric flow compared to monotonic SPCs having a highly packed pillar arrays. The density modulated column provided separation efficiencies which were superior over the monotonic minimum density (low packed) SPC and were more similar to that of maximum density SPCs. Two methods for modulating pillar density were developed and arranged in two different ways resulting in four unique DMSPC topographies. These were then compared with two control designs utilizing a minimum density of pillars and a maximum density of pillars. Of these four, Design C was shown to perform the best with regards to separation efficiency. This DMSPC performed separations on kerosene and diesel that were faster than the maximum density design under the same chromatographic conditions without any significant loss of peak resolution. This indicates that DMSPC could be used in micro GC systems for reducing the pressure requirements or in near-real-time analysis systems to reduce the time necessary for a separation to complete. Based on the experimental data, DMSPC might show an even larger advantage as the length of the separation columns increases for separation of a wider range of analytes and in more complex environments. This new column design introduces a new alternative when it comes to choosing a high performance separation column with lower pressure requirements for the use in a micro GC system.

4.7. References

[1] R. Chan, A. Lopez, B. P. Regmi, and M. Agah, "Micro-pillar density modulation in semi-packed MEMS column," in *2017 19th International Conference on Solid-State Sensors, Actuators and Microsystems (TRANSDUCERS)*, 2017, pp. 1528–1531.

[2] M. Zhou, J. Lee, H. Zhu, R. Nidetz, K. Kurabayashi, and X. Fan, "A fully automated portable gas chromatography system for sensitive and rapid quantification of volatile organic compounds in water," *RSC Adv*, vol. 6, no. 55, pp. 49416–49424, 2016.

[3] M. Akbar, M. Restaino, and M. Agah, "Chip-scale gas chromatography: From injection through detection," *Microsyst. Nanoeng.*, vol. 1, p. 15039, Dec. 2015.

[4] J. H. Sun, D. F. Cui, X. Chen, L. L. Zhang, H. Y. Cai, and H. Li, "A micro gas chromatography column with a micro thermal conductivity detector for volatile organic compound analysis," *Rev. Sci. Instrum.*, vol. 84, no. 2, p. 025001, Feb. 2013.

[5] W. R. Collin, A. Bondy, D. Paul, K. Kurabayashi, and E. T. Zellers, "μGC × μGC: Comprehensive Two-Dimensional Gas Chromatographic Separations with Microfabricated Components," *Anal. Chem.*, vol. 87, no. 3, pp. 1630–1637, Feb. 2015.

[6] H. Kim *et al.*, "A Micropump-Driven High-Speed MEMS Gas Chromatography System," in *TRANSDUCERS 2007 - 2007 International Solid-State Sensors, Actuators and Microsystems Conference*, 2007, pp. 1505–1508.

[7] C.-J. Lu *et al.*, "First-generation hybrid MEMS gas chromatograph," *Lab. Chip*, vol. 5, no. 10, pp. 1123–1131, 2005.

[8] S. K. Kim, H. Chang, and E. T. Zellers, "Microfabricated Gas Chromatograph for the Selective Determination of Trichloroethylene Vapor at Sub-Parts-Per-Billion Concentrations in Complex Mixtures," *Anal. Chem.*, vol. 83, no. 18, pp. 7198–7206, Sep. 2011.

[9] H. Shakeel, D. Wang, J. R. Heflin, and M. Agah, "Width-Modulated Microfluidic Columns for Gas Separations," *IEEE Sens. J.*, vol. 14, no. 10, pp. 3352–3357, Oct. 2014.

[10] H. Yuan *et al.*, "The effect of the channel curve on the performance of micromachined gas chromatography column," *Sens. Actuators B Chem.*, vol. 239, no. Supplement C, pp. 304–310, Feb. 2017.

[11] H. Yuan, X. Du, Y. Li, and Y. Jiang, "Mems-based semi-packed gas chromatography column with wavy channel configuration," in *2016 IEEE International Conference on Manipulation, Manufacturing and Measurement on the Nanoscale (3M-NANO)*, 2016, pp. 283–286.

[12] D. W. Armstrong, L. He, and Y. S. Liu, "Examination of ionic liquids and their interaction with molecules, when used as stationary phases in gas chromatography," *Anal. Chem.*, vol. 71, no. 17, pp. 3873–3876, Sep. 1999.

[13] L. Li, M. Wu, Y. Feng, F. Zhao, and B. Zeng, "Doping of three-dimensional porous carbon nanotube-graphene-ionic liquid composite into polyaniline for the headspace solid-phase microextraction and gas chromatography determination of alcohols," *Anal. Chim. Acta*, vol. 948, pp. 48–54, Dec. 2016.

[14] S. C. Terry, J. H. Jerman, and J. B. Angell, "A gas chromatographic air analyzer fabricated on a silicon wafer," *IEEE Trans. Electron Devices*, vol. 26, no. 12, pp. 1880–1886, Dec. 1979.

[15] M. Agah, G. R. Lambertus, R. D. Sacks, and K. D. Wise, “High-speed MEMS-based gas chromatography,” in *IEDM Technical Digest. IEEE International Electron Devices Meeting, 2004.*, 2004, pp. 27–30.
[16] M. J. de Boer *et al.*, “Micromachining of buried micro channels in silicon,” *J. Microelectromechanical Syst.*, vol. 9, no. 1, pp. 94–103, Mar. 2000.
[17] G. Lambertus *et al.*, “Design, Fabrication, and Evaluation of Microfabricated Columns for Gas Chromatography,” *Anal. Chem.*, vol. 76, no. 9, pp. 2629–2637, May 2004.
[18] M. A. Zareian-Jahromi, M. Ashraf-Khorassani, L. T. Taylor, and M. Agah, “Design, Modeling, and Fabrication of MEMS-Based Multicapillary Gas Chromatographic Columns,” *J. Microelectromechanical Syst.*, vol. 18, no. 1, pp. 28–37, Feb. 2009.
[19] H. M. McNair and E. J. Bonelli, “Basic gas chromatography,” 1969.
[20] S. Ali, M. Ashraf-Khorassani, L. T. Taylor, and M. Agah, “MEMS-based semi-packed gas chromatography columns,” *Sens. Actuators B Chem.*, vol. 141, no. 1, pp. 309–315, Aug. 2009.
[21] B. Tian *et al.*, “Research on micro-fabricated gas chromatographic columns with embedded ellipitic cylindrical posts,” in *2017 IEEE 30th International Conference on Micro Electro Mechanical Systems (MEMS)*, 2017, pp. 1343–1346.
[22] S. Nishiyama, T. Nakai, M. Shuzo, J. J. Delaunay, and I. Yamada, “Effect of micropillar density on separation efficiency of semi-packed micro gas chromatographic columns,” in *2009 IEEE Sensors*, 2009, pp. 1935–1938.
[23] H. Shakeel and M. Agah, “High density semipacked separation columns with optimized atomic layer deposited phases,” *Sens. Actuators B Chem.*, vol. 242, pp. 215–223, Apr. 2017.
[24] B. Alfeeli, S. Narayanan, M. McMillan, D. Hirtenstein, G. Rice, and M. Agah, “The effect of pillar array in semi-packed micro gas chromatography,” in *2011 IEEE SENSORS Proceedings*, 2011, pp. 1097–1100.
[25] A. D. Radadia, A. Salehi-Khojin, R. I. Masel, and M. A. Shannon, “The effect of microcolumn geometry on the performance of micro-gas chromatography columns for chip scale gas analyzers,” *Sens. Actuators B Chem.*, vol. 150, no. 1, pp. 456–464, Sep. 2010.
[26] H. Purnell, *Gas chromatography*. Wiley, 1967.
[27] B. P. Regmi, R. Chan, and M. Agah, “Ionic liquid functionalization of semi-packed columns for high-performance gas chromatographic separations,” *J. Chromatogr. A*.
[28] B. Alfeeli *et al.*, “Interchannel Mixing Minimization in Semi-Packed Micro Gas Chromatography Columns,” *IEEE Sens. J.*, vol. 13, no. 11, pp. 4312–4319, Nov. 2013.
[29] H. Shakeel, G. W. Rice, and M. Agah, “Semipacked columns with atomic layer-deposited alumina as a stationary phase,” *Sens. Actuators B Chem.*, vol. 203, pp. 641–646, Nov. 2014.

5. Conclusion

In this work, several new MEMS-based separation columns were designed and tested in an effort to create a device that decreased the pressure drop generated from standard MEMS semi-packed columns without sacrificing the separation efficiency that they provide. Each of the micro-pillar density modulated semi-packed columns showed a significant increase in total flow when compared to the maximum density control device under similar inlet pressures. At the same time, they also performed much better than the minimum density control device with regards to separation efficiency, especially at higher inlet pressures. From the new designs, the second generation ordered micro-pillar density modulated column has been shown to exhibit good performance, which can be inferred from the Van Deemter Plot that was generated. The work also identified room temperature ionic liquids for use in MEMS-based semi-packed separation columns and the methods to reliably coat these devices. These ionic liquids showed high separation efficiencies as well as increased the speed of the separations. By utilizing these two in tandem, the overall speed of separations can be increased without losing separation efficiency.

The work presented here will allow for new and exciting applications where very high speed separations or partial separations are required, especially for a portable platform. Density

modulated semi-packed columns will open up new opportunities and can be integrated into current application platforms. However, this is still not the most optimized design based off of the semi-packed column. There is always more work that can be done to optimize uSCs for specific applications. By coming up with new and creative structures, it may be possible to exceed the separation efficiency of the semi-packed columns while still reducing the pressure drop associated with them.

Another prospective avenue to direct research towards is the development of a standalone system that can differentiate between two similar test samples. Electronic noses can be utilized for this type of application [1,2] but smaller differences between samples require a lot more power in order to distinguish between. By utilizing uGC it may be possible to create a GC nose which could utilize one or more separation columns in order to make those distinctions. This is where the density modulated semi-packed columns could be used as their flow resistance is much lower than regular semi-packed columns and provide a faster overall separation. By placing these columns in parallel, and combined with the tunability of room temperature ionic liquids, it would be possible to create a very versatile platform for quickly identifying different samples as opposed to performing complete separations. This would have to work in tandem with a computing device that can perform pattern recognition as gas chromatograms are extremely complex curves that cannot be simply categorized. In fact, this is the work that will be focused on moving forward in the VT MEMS Lab on the gas chromatography side. We have already partnered with a professor from the Statistics department to develop a model in order to distinguish between different complex test mixtures. The work began using a five-channel parallel separation column with different channel topographies and two different ionic liquid stationary phases. Current work is being done to differentiate between adulterated gasoline chromatograms that have been generated

within one minute. As this is an initial study, there is much to optimize with regards to number of parallel channels, column topographies, and stationary phase. The model used to differentiate between different test mixtures will also be updated as more research has been put into the project.

One last topic that should be further explored is the method of active on chip cooling for uGC systems. With the ultimate goal of portability and point-of-care use as the motivating factor, the time that it takes for a uSC to cool down should be looked at. Long columns used in traditional GC are victims to the ovens that are used to heat them. While uSCs have a much smaller thermal mass, there can always be improvements made in order to reduce the downtime between running tests. There has already been some work done incorporating micro-channels for integrated chip cooling [3]. Applying this technology might be something that could allow for more efficient cooling for uGC systems.

Throughout the course of the work described in this thesis, I have learned a lot of new techniques and skills. Coming from a computer engineering background, there was a lot of chemistry and physics that needed to be learned in order to understand how gas chromatography worked and how fluids work at a micro vs macro scale. Some other examples include the use of various tools in the cleanroom, such as the deep reactive ion etcher, the atomic layer depositer, and the e-beam evaporator for depositing metals. Along the same lines, I learned how to operate and maintain an Agilent 7890A GC system for testing our fabricated devices as well as how to functionalize a GC separation column. I am thankful that I have also been able to work at the VT MEMS Lab as it has fostered a very close knit group of students that I can proudly call my family. While we didn't always get along, we were always able to work through our issues and return to a professional work environment.

5.1. References

[1] F. Röck, N. Barsan, and U. Weimar, "Electronic Nose: Current Status and Future Trends," *Chem. Rev.*, vol. 108, no. 2, pp. 705–725, Feb. 2008.

[2] A. Gliszczyńska-Świgło and J. Chmielewski, "Electronic Nose as a Tool for Monitoring the Authenticity of Food. A Review," *Food Anal. Methods*, vol. 10, no. 6, pp. 1800–1816, Jun. 2017.

[3] Y. Joo, K. Dieu, and C.-J. Kim, "Fabrication of monolithic microchannels for IC chip cooling," 1995.

Thesis / Dissertation Reuse

The IEEE does not require individuals working on a thesis to obtain a formal reuse license, however, you may print out this statement to be used as a permission grant:

Requirements to be followed when using any portion (e.g., figure, graph, table, or textual material) of an IEEE copyrighted paper in a thesis:

1) In the case of textual material (e.g., using short quotes or referring to the work within these papers) users must give full credit to the original source (author, paper, publication) followed by the IEEE copyright line © 2011 IEEE.
2) In the case of illustrations or tabular material, we require that the copyright line © [Year of original publication] IEEE appear prominently with each reprinted figure and/or table.
3) If a substantial portion of the original paper is to be used, and if you are not the senior author, also obtain the senior author's approval.

Requirements to be followed when using an entire IEEE copyrighted paper in a thesis:

1) The following IEEE copyright/ credit notice should be placed prominently in the references: © [year of original publication] IEEE. Reprinted, with permission, from [author names, paper title, IEEE publication title, and month/year of publication]
2) Only the accepted version of an IEEE copyrighted paper can be used when posting the paper or your thesis on-line.
3) In placing the thesis on the author's university website, please display the following message in a prominent place on the website: In reference to IEEE copyrighted material which is used with permission in this thesis, the IEEE does not endorse any of [university/educational entity's name goes here]'s products or services. Internal or personal use of this material is permitted. If interested in reprinting/republishing IEEE copyrighted material for advertising or promotional purposes or for creating new collective works for resale or redistribution, please go to http://www.ieee.org/publications_standards/publications/rights/rights_link.html to learn how to obtain a License from RightsLink.

If applicable, University Microfilms and/or ProQuest Library, or the Archives of Canada may supply single copies of the dissertation.

BACK CLOSE WINDOW

Thesis / Dissertation Reuse

The IEEE does not require individuals working on a thesis to obtain a formal reuse license, however, you may print out this statement to be used as a permission grant:

Requirements to be followed when using any portion (e.g., figure, graph, table, or textual material) of an IEEE copyrighted paper in a thesis:

1) In the case of textual material (e.g., using short quotes or referring to the work within these papers) users must give full credit to the original source (author, paper, publication) followed by the IEEE copyright line © 2011 IEEE.
2) In the case of illustrations or tabular material, we require that the copyright line © [Year of original publication] IEEE appear prominently with each reprinted figure and/or table.
3) If a substantial portion of the original paper is to be used, and if you are not the senior author, also obtain the senior author's approval.

Requirements to be followed when using an entire IEEE copyrighted paper in a thesis:

1) The following IEEE copyright/ credit notice should be placed prominently in the references: © [year of original publication] IEEE. Reprinted, with permission, from [author names, paper title, IEEE publication title, and month/year of publication]
2) Only the accepted version of an IEEE copyrighted paper can be used when posting the paper or your thesis on-line.
3) In placing the thesis on the author's university website, please display the following message in a prominent place on the website: In reference to IEEE copyrighted material which is used with permission in this thesis, the IEEE does not endorse any of [university/educational entity's name goes here]'s products or services. Internal or personal use of this material is permitted. If interested in reprinting/republishing IEEE copyrighted material for advertising or promotional purposes or for creating new collective works for resale or redistribution, please go to http://www.ieee.org/publications_standards/publications/rights/rights_link.html to learn how to obtain a License from RightsLink.

If applicable, University Microfilms and/or ProQuest Library, or the Archives of Canada may supply single copies of the dissertation.

Title: Ionic liquid functionalization of semi-packed columns for high-performance gas chromatographic separations

Author: Bishnu P Regmi,Ryan Chan,Masoud Agah

Publication: Journal of Chromatography A

Publisher: Elsevier

Date: 11 August 2017